Elucidating the Differences in the Carbon Mineralization Behaviors of Calcium and Magnesium-bearing Alumino-Silicates and Magnesium Silicates for CO_2 Storage

Greeshma Gadikota,[1] Juerg Matter,[2] Peter Kelemen,[3]

Patrick V. Brady,[4] and Ah-Hyung Alissa Park [5,6,7]*

[1]School of Civil and Environmental Engineering, Cornell University, Ithaca, NY 14853

[2]Department of Ocean and Earth Science, University of Southampton, Southampton, UK SO14 3ZH

[3]Lamont-Doherty Earth Observatory of Columbia University, Palisades, NY 10964

[4]Sandia National Laboratories, Albuquerque, NM 87123

[5]Department of Earth and Environmental Engineering, Columbia University in the City of New York, NY 10027

[6]Department of Chemical Engineering, Columbia University in the City of New York, NY 10027

[7]Lenfest Center for Sustainable Energy, The Earth Institute, Columbia University in the City of New York, NY 10027

*Corresponding Author. Phone: +1 212 854 8989. Fax: +1 212-854-7081. E-mail: ap2622@columbia.edu

Abstract

Engineering the permanent storage of CO_2 in earth-abundant Ca- and Mg-bearing silicate and alumino-silicate rocks and minerals as carbonates requires a fundamental understanding of the extents of carbonate conversion that can be achieved at conditions relevant to geologic formations. While many studies have reported the reaction rates and the carbonation extents of specific minerals, the data is limited in terms of reaction conditions and the mineral samples were relatively pure to start with. Thus, understanding of the effect of the chemical and mineralogical heterogeneity on the carbon mineralization behaviors of various minerals and rocks in geologic conditions is lacking. Therefore, this study investigated the reactivities of a selection of minerals and rocks such as (a) Mg-rich olivine ($Mg_{1.74}Fe_{0.26}SiO_4$) as previously reported by Gadikota and co-workers (2014),[1] labradorite (plagioclase feldspar with $Ca_{0.53}Na_{0.47}Al_{1.53}Si\ O_8$), (b) anorthosite (a mixture of plagioclase ($Ca_{0.98}Na_{0.02}Al_{1.98}Si_{2.02}O_8$), olivine ($Mg_{1.32}Fe_{0.68}SiO_4$) and magnetite ($Fe_3O_4$)), and (c) basalt (a fine-grained volcanic rock containing a mixture of plagioclase ($Ca_{0.6}Na_{0.4}Al_{1.6}Si_{2.4}O_8$), calcic pyroxene (~$Mg_{0.48}$, $Fe_{0.52}CaSi_2O_6$) and low Ca pyroxene (~$Mg_{0.48}Fe_{0.52}SiO_3$)), that are relevant to CO_2 storage. The reaction conditions were also selected to mimic the conditions relevant to geologic CO_2 storage sites (T_{max} = 185ºC, P_{max} = 164 bar, 0 - 1 M $NaHCO_3$, 0 - 1 M NaCl, 1.0 M NaCl + 0.64 M $NaHCO_3$). Our studies show that the extents of carbonation of olivine, labradorite, anorthosite, and basalt are 85, 35, 19 and 9%, respectively, when reacted for three hours at 185 ºC, P_{CO2} of 139 atm in 1.0 M NaCl + 0.64 M $NaHCO_3$ with 15 wt% solid reactant and a stirring rate of 800 rpm. Further, our results indicate that increasing the reaction temperature over the range of 90 to 185 °C, and increasing the concentration of $NaHCO_3$ over the range of 0 to 1 M, both enhance the extent of carbon mineralization. On the other hand, increasing the partial pressure of CO_2 from 64 atm to 169 atm and raising the concentration of NaCl to 1.0 M have no significant effects within the time-scale of these experimental studies. Comparison of our results with previous studies suggests that the reactivity of Ca- and Mg-bearing alumino-silicates is lower compared to Ca- and Mg-bearing silicates.

Keywords: carbon mineralization, alumino-silicates, silicates, calcium carbonate; magnesium carbonate

1. Introduction

Global reliance on fossil energy resources has spurred an increase in CO_2 emissions. The need to sustainably produce and use our energy resources has motivated us to explore the potential storage of CO_2 in geologic formations. Further, the conversion of CO_2 to water insoluble calcium and magnesium carbonates in the subsurface environments may reduce the potential cost of monitoring the fate of mobile CO_2. However, there is a limited understanding of the reactivity of CO_2 with calcium and magnesium-bearing materials to directly form calcium and magnesium carbonates in the subsurface environments. The conversion of CO_2 to calcium or magnesium carbonates is a thermodynamically downhill pathway for permanently storing CO_2. Estimates have shown that more than 10,000 - 1,000,000 gigatons of carbon can be sequestered by converting CO_2 to carbonates,[2] which is also known as carbon mineralization. One of the key advantages of forming calcium and/or magnesium carbonates is that they are relatively insoluble in water and thermodynamically stable at Earth's surface conditions.[1,3,12–17,4–11]

While natural, rock-forming calcium and magnesium silicates and alumino-silicates are abundant and available for the conversion of CO_2 to calcium and magnesium carbonates,[2,3,18] the kinetics of direct conversion to carbonates in an environment characterized by CO_2 - reaction fluid - calcium and magnesium-bearing silicates and alumino-silicates are not very well understood. A fundamental understanding of these kinetics is essential for developing subsurface technologies for accelerated carbon storage in geologic environments and for designing engineered processes to convert Ca- and Mg-bearing materials to their respective carbonates. The Ca- and Mg-bearing materials of interest include minerals such as olivine ($(Mg,Fe)_2SiO_4$)), wollastonite ($CaSiO_3$), pyroxenes $(Mg,Fe,Ca)_2Si_2O_6$, and plagioclase feldspar (solid solution from albite, $NaAlSi_3O_8$ to anorthite, $CaAl_2Si_2O_8$). These minerals and their amorphous equivalents are abundant in rocks such as peridotite (> 40% olivine), gabbros and anorthosites (mixtures of plagioclase, olivine and pyroxenes) and basalt (volcanic equivalent of gabbro, rich in Mg and Ca), and industrial residues such as asbestos, mining wastes, steel slags, and cement kiln dust.

Various studies have shown that industrial residues such as fly ash,[19–25], asbestos,[15,26–28], steel slags,[29–35] and cement kiln dust[36,37] can be converted to calcium and/or magnesium bearing carbonates within a few hours. However, the time scales for the conversion of more abundant, rock-forming minerals have not been systematically investigated. Further, the reactivities of heterogeneous natural Ca- and/or Mg-alumino-silicate or silicate-bearing materials such as labradorite, anorthosite, and basalt have not been benchmarked against more reactive materials such as olivine. Laboratory-scale studies have shown that carbonate conversions above 80% are achieved when olivine or wollastonite are reacted in an environment comprising supercritical CO_2 (P_{CO2} ~ 150 atm), reaction fluid (water in case of wollastonite, and 1.0 M NaCl + 0.64 M $NaHCO_3$), and at temperatures greater than 90 ^oC.[7]

Another challenge in determining the reactivities of Ca- and Mg-bearing silicates and alumino-silicates is the determination of the appropriate rate law for estimating the conversion of CO_2 to carbonates. In coupled CO_2 - reaction fluid – mineral or rock environments, the conversion of CO_2 to carbonates proceeds through the dissolution of CO_2 in the fluid[38,39] (Reactions 1-3), followed by the dissolution of the mineral or rock [40,41,50–59,42,60–62,43–49] (Reactions 4-5) and the formation of Ca-or Mg-carbonates (Reactions 6-7).[63–65]

CO_2 hydration: $2CO_{2\,(g)} \rightarrow 2CO_{2\,(aq)}$ (Reaction 1)

$$2CO_{2\,(aq)} + 2H_2O \leftrightarrow 2H_2CO_{3\,(aq)} \leftrightarrow 2H^+_{(aq)} + 2HCO^-_{3\,(aq)} \quad \text{(Reaction 2)}$$

$$2HCO^-_{3\,(aq)} \leftrightarrow 2CO^{2-}_{3\,(aq)} + 2H^+_{(aq)} \quad \text{(Reaction 3)}$$

Olivine Dissolution: $(Mg,Fe)_2SiO_{4(s)} + 4H^+_{(aq)} \rightarrow 2Mg^{2+}_{(aq)} + 2Fe^{2+}_{(aq)} + SiO_{2\,(aq)} + 2H_2O$ (Reaction 4)

Anorthite Dissolution: $CaAl_2Si_2O_{8(s)} + 8H^+_{(aq)} \rightarrow Ca^{2+}_{(aq)} + 2Al^{3+}_{(aq)} + 2SiO_{2(aq)} + 4H_2O$ (Reaction 5)

Carbonate Formation: $Mg^{2+}_{(aq)} + CO^{2-}_{3\,(aq)} \rightarrow MgCO_{3\,(s)}$ (Reaction 6)

$$Ca^{2+}_{(aq)} + CO^{2-}_{3\,(aq)} \rightarrow CaCO_{3\,(s)} \quad \text{(Reaction 7)}$$

The rate-limiting step in carbon mineralization is typically assumed to be the dissolution reaction. More recent studies have indicated that coupling the dissolution and carbonation steps while tuning the pH conditions enhances the mineralization behavior.[1] Laboratory scale studies by Gadikota et al., (2014)[1] and NETL-Albany[7,66–68] have shown that carbon mineralization of the ground powders of magnesium and calcium bearing silicates and alumino-silicates can be achieved over a time-scale of a few hours, while Schaef and co-workers[69,70] showed that basalt grains can be converted to carbonates over the course of a few days. These observations are supported by field-scale evidence of basalt carbonation through the CarbFix Project in Icelend.[71] Other factors that impact carbon mineralization behavior include the morphological changes and the resulting feedbacks on the reactivity of the mineral or rock. The formation of diffusion limiting passivation layers of silica and iron oxide during the conversion of olivine to magnesium carbonate has been reported.[1,72–74] Crystallization of other diffusion limiting phases such as gibbsite ($Al(OH)_3$) and kaolinite ($Al_2Si_2O_5(OH)_4$) has been reported during the carbonation of plagioclase ($Ca_{1-x}Na_xAl_{2-x}Si_{2+x}O_8$).[75] More recently, Hellevang and co-workers reported the formation of smectite during basalt carbonation.[76] Extensive carbonate growth on olivine grains has been shown to reduce the porosity by an order of magnitude.[1]

Another challenge in this research area is the lack of systematic studies investigating the effect of temperature on plagioclase-bearing rocks and minerals, in contrast to studies of more reactive minerals such as olivine, serpentine, and wollastonite.[5–7,43,67,77,78] Increasing the temperature aids faster dissolution of olivine, plagioclase, and basalt [40,41,59,61,79,43,47,49,54–58] and reduces the solubility of calcite and magnesite,[80–82] thereby aiding the overall extents of carbon mineralization. However, a comparison of the effect of temperature on the direct carbon mineralization behaviors of labradorite, and basalt has not yet been reported.

Other parameters that influence carbon mineralization behaviors are the partial pressure of CO_2 and the composition of the reaction fluid, particularly the pH of the system. In deionized water and in the absence of a pH buffer, pressurized CO_2 dissolves in water to produce a pH around 3,[49] which causes rapid

dissolution of the alkaline calcium and magnesium bearing silicate and aluminum silicate minerals. The resulting depletion of H^+ ions and increasing concentration of alkaline species in solution increases the pH of the CO_2-water-mineral system to aid the formation of carbonates.[1,8] However, the presence of additives such as $NaHCO_3$ that serve as a carbon carrier and buffer the solution pH in the range of 6-8 has been shown to aid the direct carbonation of olivine, serpentine, and wollastonite.[1,7,67,77,83] The role of $NaHCO_3$ on the carbon mineralization of plagioclase-bearing minerals and rocks such as labradorite, anorthosite, and basalt has not been reported in the literature. Non-buffering additives such as NaCl have been shown to aid mineral dissolution[67] through the complexation of Cl^- with the cations, but do not have a significant effect on the overall mineralization behavior of olivine.[1,84] The effect of varying NaCl concentrations on the extents of carbonation of plagioclase, and plagioclase-bearing rocks, has not been reported.

As discussed here, there are large gaps between available experimental data and information that are needed to better predict the *in-situ* carbon mineralization behaviors during the geologic injection and storage of CO_2. Thus, the aim of this study is to obtain and present experimental data relating the reactivity and morphological behaviors of plagioclase ($Ca_{1-x}Na_xAl_{2-x}Si_{2+x}O_8$) bearing minerals and rocks such as labradorite (plagioclase feldspar with $Ca_{0.53}Na_{0.47}Al_{1.53}Si_{2.47}O_8$), anorthosite (a mixture of plagioclase ($Ca_{0.98}Na_{0.02}Al_{1.98}Si_{2.02}O_8$), olivine ($Mg_{1.32}Fe_{0.68}SiO_4$) and magnetite ($Fe_3O_4$)) and basalt (a fine-grained volcanic rock containing a mixture of plagioclase ($Ca_{0.6}Na_{0.4}Al_{1.6}Si_{2.4}O_8$), calcic pyroxene (~$Mg_{0.48}$, $Fe_{0.52}CaSi_2O_6$) and low Ca pyroxene (~$Mg_{0.48}Fe_{0.52}SiO_3$)) at elevated reaction temperatures (90-185 ºC) and partial pressures of CO_2 (64-164 atm), with fluids containing $NaHCO_3$ (0.0 - 1.0 M), and NaCl (0.0 - 1.0 M). These results are compared to previously published reactivities of minerals and rocks under similar experimental conditions[1,77,85] to quantitatively constrain the choice of minerals and rocks for natural and accelerated conversion of CO_2 to solid carbonates in geologic formations.

2. Experimental Methods

2.1 Procurement and Characterization of Materials

Labradorite from the Norcross-Madagascar Mine in the south of Madagascar and procured from the Madagascar Mineral Company as a fine powder. The anorthosite sample obtained from the DOE Albany Research Center is originally from Grass Valley, California. Columbia River Basalt, also from the Albany Research Center, is a light gray, fine grained basalt from a vesicular core from a depth of 2263.3 feet. The studies reported here are compared with results of experiments performed on Twin Sisters olivine at the same conditions, reported in a previous publication. Freshly ground mineral and rock samples were used since our previous studies[1,84] and those reported by Eggleston and co-workers[86] showed that aging the ground mineral powders reduces their reactivity.

The mineral and rock samples are ground such that more than 90% of the material is smaller than 37 μm. The mean particle diameters of labradorite, anorthosite, and basalt, determined using laser diffraction (Beckman Coulter, Inc., LS 13 320 MW) are 8.44, 11.94, and 7.81 μm, respectively. The specific surface areas determined using the BET technique (Quantachrome NovaWin BET Analyzer) are 4.46, 2.92, and 4.48 m^2/g, respectively. The BET technique is based on multilayer adsorption in which the non-reactive gases are used to adsorbates to quantify the specific surface area and porosity of materials. The elemental compositions in rocks and minerals are determined using Wavelength Dispersion X-Ray Fluorescence (WD-XRF, Pananalytical Axios). CaO content in anorthosite (14.10 wt%) is the highest followed by labradorite (10.2 wt%), basalt (8.15 wt%) and olivine (0.16 wt%). MgO content in olivine (47.3 wt%,)[1] is the highest, followed by anorthosite (8.74 wt%), basalt (4.82 wt%), and labradorite (0.24 wt%) (Table 1). On the basis of a CIPW norm calculation, we estimate that the anorthosite sample contains about 66 wt% plagioclase feldspar (96 mol% anorthite, $CaAl_2Si_2O_8$ + 4 mol% albite, $NaAlSi_3O_8$, abbreviated An96), 24% olivine (66 mol% forsterite, Mg_2SiO_4 + 34 mol% fayalite, Fe_2SiO_4), 5% calcic pyroxene and 3% iron-titanium oxide minerals. Similarly, the basalt used in this study contains about 55% plagioclase (An61), 16% calcic pyroxene, 22% Ca-lean pyroxene (both pyroxenes with molar Mg/(Mg+Fe) ~ 0.49), and 7% iron-titanium oxides.

2.2. Carbonation of Minerals and Rocks and Analyses of Reaction Products

The carbonation experiments are performed in a high temperature, high pressure batch reactor (Autoclave Engineers, 100 ml EZE-Seal) as discussed in our previous publication.[1] To summarize, a high pressure syringe pump (Teledyne Isco, 500D, NE) for delivering pressurized CO_2 is connected to the reactor. The slurry is composed of 15 wt% solids suspended in the reaction fluid containing deionized water and/or aqueous fluids with varying concentrations of NaCl (0.0 - 1.0 M) and $NaHCO_3$ (0.0 - 1.0 M). Once the reactor is sealed and the set-point of the reaction temperature is reached after about 40 minutes, the reactor pressure is increased to the desired partial pressure of CO_2, which marks the start of the experiment. At the end of the experiment, the reactor is cooled to temperatures below 70 ºC, which takes about 75 minutes. The reactor is then depressurized, the interior is cleaned to collect all the solid material, and the fluid contents are filtered. The filtered liquid samples are diluted in 2% HNO_3 and the concentrations are measured using Inductively Coupled Plasma - Atomic Emission Spectroscopy (ICP-AES, Activa S model, Horiba Jobin Yvon).

In addition to the liquid analyses, a host of tests are conducted on the solids which include the determination of the porosity and the specific surface area using BET (Brunauer–Emmett–Teller, Quantachrome NovaWin BET Analyzer), the particle size via laser diffraction (Beckman Coulter, Inc., LS 13 320 MW), and changes in the surface morphological features using Scanning Electron Microscopy (SEM, Tescan Vega II). These tests provide insight into the morphological changes in the solids before and after carbonation. In addition, the crystalline phases in the unreacted and reacted minerals and rocks are identified using X-Ray Diffraction (XRD 3000, Inel Inc.) in the range of 20º and 80º with CuKα radiation (λ = 1.5406 Å).

2.3. Quantification of Mineralized CO_2

The determination of the carbon content in the reacted samples is complicated by the relatively low content of carbon in reacted labradorite, anorthosite and basalt. The carbon content is measured using

Thermogravimetric Analysis (TGA, Setaram SETSYS) and Total Carbon Analysis (TCA, UIC CM150) with a heating rate of 5°C per minute. Total Inorganic Carbon (TIC) analysis using acid digestion is not used to measure the carbon content in the samples because the samples do not contain any organic carbon, and TIC is much slower than TCA.[1] While the TGA can be used to determine the presence of various phases (e.g., hydroxides, carbonates) based on their decomposition temperature, the presence of overlapping weight drop curves makes it challenging to accurately determine phase proportions, especially for experiments in which the carbonate content is low. In the TCA where the samples were combusted to convert all organic and inorganic carbon to CO and CO_2, the detection of small amounts of carbon is more accurate (see Table S1 for CO_2 content in the reacted minerals and rocks). The following equation is used to estimate the extent of carbonation using TCA:

$$Y_{CO_2,TCA} = R_{CO_2} \times \left(\frac{3.67 \times TCA}{(1 - 3.67 \times TCA)}\right) \times 100\% \quad \text{(Eq. 1)}$$

where Y_{CO_2}, the yield or the extent of carbonation is then defined as the measured amount of CO_2 stored in the mineral as solid carbonate relative to the CO_2 storage capacity, $\frac{1}{R_{CO_2}}$, the theoretical carbon storage capacity is the mass of CO_2 that can be trapped in a unit mass of the unreacted mineral, and *TCA* represents the weight fraction of carbon in the carbonated sample with a unit of $\left[\frac{Weight\ of\ carbon}{Weight\ of\ solid\ sample}\right]$. The coefficient 3.67 is the ratio of the molecular weights of CO_2 to C. The extents of carbonation are reported assuming that the magnesium and calcium content in the minerals and rocks reacts with CO2 to form magnesium and calcium carbonates. The role of iron and sodium are not considered.

$$\frac{W_{CO_2}}{W_{mineral}} = \frac{1}{R_{CO_2}} = \left(\frac{y_{Mg}}{MW_{Mg}} + \frac{y_{Ca}}{MW_{Ca}}\right) \times MW_{CO_2} \quad \text{(Eq. 2)}$$

The possible formation of Na, K and Al carbonates is not considered in our estimates of carbon storage capacity since Na and K form soluble carbonates and the formation of aluminum carbonates is not evident in the carbonated samples, as expected for these highly soluble minerals in our experiments at high water/rock ratio. In natural systems with Na-rich plagioclase, the carbon storage capacity could be substantially increased if Na- and K-carbonate saturation was achieved.

3. Results and Discussion

3.1 Effect of Reaction Time

Insights into the kinetics of the carbonation of olivine and plagioclase-bearing minerals and rocks can be obtained by determining the effect of reaction time which was investigated at 1, 3, and 5 hours, at a reaction temperature of 185 ºC, P_{CO2} of 139 atm (P_{total} = 150 atm) in 1.0 M NaCl + 0.64 M $NaHCO_3$ with 15 wt% solid and a stirring rate of 800 rpm (**Figure 1 (a)**).These conditions are the same as those reported for our previous carbon mineralization studies with olivine [1] and similar to those of NETL-Albany.[7,67] The extents of carbonation are calculated based on the formation of calcium and magnesium carbonates. For olivine and labradorite, the extent of carbonation continues to increase with reaction time, up to five hours. The extents of olivine carbonation are 57, 85 and 90% for reaction times of 1, 3 and 5 hours, respectively. With the same time increments, the extents of labradorite conversion are 11, 35, and 46 %. Despite some expectations that reaction rates might decrease over time, due to early consumption of the smallest grains and/or passivation of reactive surfaces, our experimental data for both of these minerals can be approximately fit with a constant rate of consumption, ≥ 35% per hour for olivine, and about 12% per hour for labradorite (**Figure 1(b-1) and 1(b-2)**). Moreover, our data for olivine are supported by data from other labs, using similar experimental conditions.[67,83]

In contrast, anorthosite and basalt conversion to carbonates slow down significantly after three hours of reaction. Anorthosite and basalt conversions in the first hour are 7% and 8%, respectively. Anorthosite conversion is 20% at both 3 and 5 hours. Basalt conversion increases very slightly from 9% to 10% on increasing the reaction time from 3 to 5 hours. These data support the hypothesis that consumption of the smallest, most reactive grains, and passivation, yield incomplete carbonation of some materials. The observation that pure minerals (olivine, plagioclase) do not exhibit this behavior, while mixtures do, suggests a role for Mg- and Al-bearing clay minerals in the passivation process, with Mg derived from olivine and pyroxenes, and Al derived from plagioclase feldspar.

Liquid analyses for labradorite experiments showed that the Ca concentrations in the solution are 10.5, 8.2, and 4.4 ppm at the end of 1, 3, and 5 hours, respectively. Similarly, the liquid analyses for anorthosite showed that the concentrations of Ca and Mg were 7.6, 5.1, 2.7 ppm and 2.5, 1.8, 0.9 ppm, respectively at the end of 1, 3, and 5 hours. The Ca and Mg concentrations for basalt are 3.4, 1.6, 0.7 ppm and 1.2, 0.7, 0.3 ppm, respectively at the end of 1, 3, and 5 hours. In dissolution only cases, the concentrations of Ca and Mg are expected to increase over time. However, the decrease in the concentrations of Ca and Mg over time indicates that as the minerals and rocks dissolve, Ca and Mg are readily precipitated in carbonate minerals. These data suggest that the dissolution of the minerals is the rate-limiting step in the direct carbonation of olivine- and plagioclase-bearing minerals and rocks to form carbonates. Together with carbonate precipitation, a contributing factor in the progressive decrease in the concentrations of Ca and Mg could be formation of passivation layers that reduce the reactivity of these minerals and rocks.

3.3 Effects of Partial Pressure of CO_2

Carbon mineralization of plagioclase-bearing minerals and rocks is important to investigate since high CO_2 partial pressures in the range of 100-150 atm are injected into plagioclase-rich geologic storage sites after CO_2 capture and compression. Therefore, many studies have focused on understanding high pressure CO_2-mineral-reaction fluid interactions[1,7,43,67,75,77,87]. In this study, the extents of carbon mineralization are investigated at CO_2 partial pressures of 64, 89, 139 and 164 atm, while other reaction parameters are held constant (185 ºC, 1.0 M NaCl + 0.64 M $NaHCO_3$, 3 hours, 15 wt% solid, 800 rpm stirring).

The extents of carbon mineralization of labradorite, anorthosite, and basalt are in the range of 33-39%, 18-20%, and 8-10% respectively, independent of P_{CO2} (**Figure 2(a) and Table 2**). These results suggest that varying CO_2 partial pressures in the range of 64-164 atm is not the rate-limiting step in the mineralization process. Unlike plagioclase, and plagioclase-bearing rocks, olivine is more sensitive to the changes in the CO_2 partial pressure. At CO_2 partial pressures of 64, 89, 139 and 164 atm, extents of olivine carbonation are 39, 60, 85, and 84%, respectively.[1] At 64 atm and 185ºC, the vapor density of CO_2 is 80 kg/m^3. At the

same temperature of 185ºC and higher pressures of 89, 139, and 164 atm, the density of supercritical CO_2 is 110, 180, and 220 kg/m^3, respectively. While CO_2 partial pressures and densities in the range of 89-164 atm is well-correlated with the higher reactivity of olivine up to 139 atm (**Figure 2(b)**), the corresponding effects on the mineralization of plagioclase-bearing minerals and rocks is not very significant.

In contrast with our experimental results, plagioclase carbonation studies performed by Munz and co-workers[75] show greater sensitivity of mineralization to pressure. Their experiments were performed with an average grain size of 10 μm in deionized water over 24 hours at 200 ºC, and resulted in 16% carbonation at P_{CO2} of 100 bar and 7% carbonation at P_{CO2} of 40 bar.[75] In contrast, we achieve extents of labradorite mineralization as high as 35% and 46% within 3 and 5 hours of reaction time, respectively. One significant point of difference between the results reported and those reported by Munz and co-workers[75] is the solution chemistry. Our experiments are performed in 1.0 M NaCl + 0.64 M $NaHCO_3$, while the experiments reported by Munz and co-workers[75] used deionized water. In the absence of a buffer such as $NaHCO_3$, high P_{CO2} in water leads to a low pH which favors dissolution as opposed to the formation of carbonates. In our experiments, the pH is buffered by dissolving $NaHCO_3$, and there is little change in pH with changing P_{CO2} based on PhreeqC simulations.

In order to determine the effect of the partial pressure of CO_2 on the in-situ pH of the solution over the course of the reaction, PhreeqC simulations were performed for anorthite ($CaAl_2Si_2O_8$). The equilibrium pH values of the solution are 6.69, 6.55, 6.35, and 6.27 respectively at partial pressures of CO_2 of 64, 89, 139, and 164 atm, respectively. Since the pH is not too high or low and the changes in the pH are small over CO_2 partial pressures in the range of 64-164 atm, dissolution of reactants and precipitation of carbonates are both favored in our experiments. PhreeqC simulations with olivine reported in a previous study also showed that the pH is in the range of 6-7.[1]

3.4 Effects of Reaction Temperature

While holding the partial pressure of CO_2 constant at 139 atm, the effect of temperature on the mineralization behavior of plagioclase-bearing minerals is investigated. As reviewed by Palandri & Kharaka (2004), and confirmed by more recent work,[43,49,60–62] studies have shown that increasing the reaction temperature enhances the dissolution rates of olivine and plagioclase. Another factor that aids the formation of magnesium and calcium carbonates at higher temperatures, is the reduced carbonate solubility with temperature.[89] However, the effects of temperature on coupled dissolution and carbonation behavior of anorthosite, labradorite, and basalt have not been reported extensively. As in our previous olivine carbonation studies[1], our experiments with anorthosite, labradorite, and basalt are performed in a solution of 1.0 M NaCl + 0.64 M $NaHCO_3$ at P_{CO2} = 139 atm for 3 hours with 15 wt% solid and at a stirring rate of 800 rpm.

The extents of carbonation of labradorite and anorthosite carbonation are 13.9, 14.1, 25.6, 35.3% and 5.9, 6.9, 10.3, 19.3% at 90, 125, 150 and 185 ºC, respectively (**Figure 3**). The correlation between temperature and the extent of carbonation at temperatures is similar to olivine carbonation behavior.[1,7] However, increasing the reaction temperature from 90ºC to 185ºC has a much smaller effect on the extent of basalt carbonation. The extents of basalt carbonation are 5.5, 7.1, 7.7, 8.6% at 90, 125, 150 and 185 ºC, respectively. The slower reactivity of the plagioclase-bearing minerals and rocks relative to ultramafic minerals such as olivine is attributed to the slower dissolution rates of plagioclase (see data compiled by Kelemen and co-workers[84]) and passivation from the precipitation of secondary phases such as smectite [75,76,87] limiting mass transfer.

3.5 Effect of $NaHCO_3$ and NaCl

In addition to the effect of temperature, the composition of the reaction fluid is another important factor that impacts carbon mineralization behavior. Various studies have engineered the chemistry of these solutions to tune the *ex-situ* conversion of Ca- and Mg-bearing materials to carbonates[2,7,8,16,67] as reviewed

by Kelemen and co-workers.[84] In *in-situ* environments, the fundamental effect of pH and salinity on the direct mineralization of plagioclase-bearing minerals is not as well understood, unlike other minerals such as olivine[1,67,77,83] and wollastonite.[16] Previous experimental studies of the effect of $NaHCO_3$ on the carbon mineralization behavior of olivine established that $NaHCO_3$ is a pH buffer and a carbon carrier during direct mineralization.[1,67,77,83] A similar experimental methodology is applied to investigate the effect of $NaHCO_3$ on the carbon mineralization behavior of plagioclase-bearing minerals and rocks. In this study, the experiments are performed at 185 °C, P_{CO2} of 139 atm for 3 hours, with 15 wt% solid and a stirring rate of 800 rpm, the same conditions as in our previously published olivine carbonation experiments.[1]

The extents of labradorite, anorthosite and basalt carbonation are 4.8, 8.4, 11.6, 22.9%; 7.7, 8.2, 10.4, 25.8 % and 3.5, 7.8, 10.4, and 14.5% in deionized water, 0.48, 0.64, and 1.0 M $NaHCO_3$, respectively, all increasing by a factor of 3 to 5 over this range of fluid composition (**Figure 4(a)**). Unlike these plagioclase-bearing minerals and rocks, the extents of olivine carbonation are much more sensitive to changes in $NaHCO_3$ concentration. In deionized water, 0.48 M, 0.64 M, and 1.0 M $NaHCO_3$, the extents of olivine carbonation are 5.8, 56.0, 82.7, and 85.0%, respectively, increasing by a factor of ~ 15.[1] Higher extents of olivine carbonation with increasing concentration of sodium bicarbonate are consistent with the data reported by Chizmeshya and co-workers.[77]

To investigate the differences in the extents of carbonation of olivine vs. the other alumino-silicate bearing minerals and rocks, we used PhreeqC[90] to predict the equilibrium solution pH and the carbonate concentration in varying $NaHCO_3$ concentrations at 185°C and P_{CO2} = 139 atm in pure minerals: forsterite (Mg_2SiO_4) and anorthite ($CaAl_2Si_2O_8$) as a proxy for the other mineral phases. PhreeqC simulations showed significant differences in the pH and dissolved carbonate concentration of anorthite-CO_2-reaction fluid system with and without $NaHCO_3$. The equilibrium pH for an anorthite-CO_2-reaction fluid system increased from 4.03 in deionized water to 6.36, 6.49 and 6.69, and that of dissolved carbonate concentrations from 5.7×10^{-10} mol/kg to 2.5×10^{-4}, 5×10^{-4} and 1.5×10^{-3} mol/kg in 0.48, 0.64 and 1.0 M $NaHCO_3$, respectively. In comparison, the equilibrium pH for an olivine-CO_2-reaction fluid system increased from 5.42 to 6.37,

6.49, 6.69 in deionized water, 0.48 M, 0.64 M, and 1.0 M $NaHCO_3$. These data suggest that the concentration of carbonate ions, particularly at high concentrations of $NaHCO_3$, is not the limiting factor on the carbon mineralization of plagioclase-bearing rocks and minerals. Other factors, such as slower dissolution kinetics of plagioclase and plagioclase-bearing rocks, and passivation via precipitation of secondary mineral phases such as clay minerals[75,76] may be the reasons why the extent of carbonation of plagioclase-bearing minerals or rocks is not as high as that of olivine.

The role of salinity on the carbon mineralization behavior of plagioclase-bearing minerals is another important consideration since most proposed sites for geologic storage of CO_2 contain saline aqueous fluids ("brine") in pore space. These experiments are performed at 185 ^{o}C, P_{CO2} of 139 atm for 3 hours, with 15 wt% solid and a stirring rate of 800 rpm, for direct comparison with our results using olivine.[1] The extents of anorthosite carbonation in deionized water and NaCl are greater than those of labradorite and basalt. This may be due to the content of more reactive minerals such as olivine in anorthosite compared to basalt or labradorite. The extents of anorthosite and basalt carbonation are 7.7, 7.2, 8.5 % and 3.5, 4.2, 5.7% in deionized water, 0.5 M and 1.0 M NaCl, respectively (**Figure 4(b)**). The extents of labradorite carbonation are 4.8, 3.9, and 3.4% in deionized water, 0.5 M, and 1.0 M NaCl (**Figure 4(b)**). In contrast, the extent of carbon mineralization in olivine increased from 6% in deionized water to 14% in 1.0 M NaCl.[1]

Many studies have investigating the effect of NaCl on mineral carbonation. While some studies suggest that Cl^- enhances dissolution by binding to cations such as Mg or Ca,[67] others suggest that NaCl increases the ionic strength and reduces the solubility of CO_2,[91] which in turn limits the carbonate ions available to form $CaCO_3$ or $MgCO_3$. Olivine dissolution studies have shown that adding salt changes the pH, which in turn may affect dissolution[92] and that changing the ionic strength alters the crystal structure of magnesite.[93] Thermodynamic calculations using PhreeqC have shown that the equilibrium pH of the anorthite - CO_2 - NaCl system at the reaction conditions is 3.94 for NaCl concentrations in the range of 0 - 1.0 M NaCl, which aids silicate dissolution but not carbonate precipitation. In the presence of a pH buffer and carbon carrier such as $NaHCO_3$, the pH is in the range of 6-7, which aids both dissolution and carbonation.

As reported in our previous studies,[1] the presence of NaCl alone, and the absence of $NaHCO_3$ prompts the precipitation of iron oxide on reacting olivine surfaces. The formation of an iron oxide layer is evident in experiments on iron-rich minerals or rocks such as anorthosite, basalt and olivine. The precipitation of iron oxide during carbon mineralization was also reported in previous studies.[93,94] While the precipitation of iron oxide is often visible in minerals and rocks that have a high content of iron and when reacted in the absence of a pH buffer such as $NaHCO_3$, often it is difficult to determine this phase using XRD alone due to the amorphous character of these materials. In addition to the precipitation of passivating phases such as iron oxide, other factors such as the reduced solubility of CO_2, limited availability of the carbonate ions, and lower equilibrium pH values in saline environments may contribute to the lower extents of carbonation in plagioclase and plagioclase-bearing rocks, compared to olivine.

3.6 Morphological and Phase Changes due to Mineral Carbonation

In natural geologic environments, the feedbacks between the phase changes from carbon mineralization and the morphological changes have important implications for the changes in the porosity and surface area. To investigate changes in morphology, particle size, surface area, and porosity of the unreacted material were compared with the properties of reaction products, after reaction for 3 hours at 185 ^{o}C, P_{CO2} = 139 atm in 1.0 M NaCl + 0.64 M $NaHCO_3$ with 15 wt% solid and a stirring speed of 800 rpm. At these experimental conditions, the extents of labradorite, anorthosite, and basalt carbonation are 35.3, 19.3, and 8.6%, respectively compared to 85% of olivine conversion.[1] For these extents of carbonation, the average particle diameter was found to increase by 25% in labradorite, anorthosite, and basalt (**Table 3**). At similar experimental conditions, the particle diameter of olivine increased by 28%. This increase in the average particle diameter is attributed to consumption of smaller reactant grains, growth of carbonates, and precipitation of secondary phases such as clays. Further, the surface areas of labradorite, anorthosite, and basalt decreased by 38, 38, and 19%, respectively, during carbon mineralization (**Table 3**). These reductions in the surface area are much smaller than the four-fold reduction in surface area of olivine on carbonation.[1]

The changes in surface area are closely related to the changes in the cumulative pore volume. For example, **Figure 5** shows that in the case of olivine, which has the highest extent of carbonation, an order of magnitude reduction in the cumulative pore volume is noted after carbonation. Pore volume profiles of anorthosite and labradorite are similar in that there is a significant reduction in the micro and mesopores but not in the macropores. The cumulative pore volume of reacted basalt is virtually unchanged compared to the unreacted solid. This is presumably due to the low extent of basalt carbonation compared to the other minerals and rocks. The lower extents of carbonation in plagioclase and plagioclase-bearing rocks relative to olivine are also captured in the SEM images. The extensive growth of magnesite in olivine is clearly evident in **Figure 6 (a)**, compared to the sparse growth of carbonates in the plagioclase-bearing minerals and rocks (**Figures 6 (b), (c), and (d)**). These data are supported by the observations of various phases in X-Ray Diffraction (XRD) (**Figures S1 (a), (b) and (c)**). However, the calcite and magnesite phases are not very prominent given the relatively low abundance of these phases in the reacted materials.

The reduced reactivity of plagioclase-bearing minerals and rocks during carbonation has been attributed to precipitation of clay minerals such as smectite ($(Na,Ca)(Al,Mg)_6(Si_4O_{10})_3(OH)_6{\cdot}nH_2O$) and kaolinite ($Al_2Si_2O_5(OH)_4$).[75,76,87] Equilibrium simulations, using the PhreeqC software[90] with the LLNL database, also predict precipitation of magnesium-bearing clay minerals such as sepiolite during the carbonation of anorthite ($CaAl_2Si_2O_8$) and forsterite (Mg_2SiO_4) mixtures to represent anorthosite. Our results also suggest the precipitation of clays such as smectite ($(Na, Ca)_{0.3}(Al, Mg)_2(Si_4O_{10})(OH)_2.\ nH_2O$) during labradorite and basalt carbonation and Mg-based clays such as sepiolite ($Mg_4Al_2Si_{10}O_{27}.15H_2O$) during anorthosite carbonation. Smectite precipitation in reacted labradorite and basalt are consistent with the results reported by Hangx and co-workers[87] and Hellevang and co-workers,[76] respectively. These precipitated clays may be potentially diffusion limiting, which could be attributed to the reduced reactivity of plagioclase and plagioclase-bearing rocks. Another factor that potentially contributes to the low reactivity of basalt is the crystalline nature of the basalt sample we used. Glassy basalts are farther from equilibrium with water, and have much higher experimental dissolution rates than crystalline basalts (e.g., data of Gislason & Oelkers,

2003,[55] plotted in Kelemen et al., 2011, Figure 5[84]). Glassy basalts are thus expected to have higher carbonation rates compared to crystalline basalt.

4. Implications for Engineered CO_2 Storage via *in-situ* and *ex-situ* Mineralization

One of the challenges in deploying carbon mineralization at scale is the identification of the appropriate minerals or rocks for *ex-situ* and *in-situ* conversion of CO_2 to carbonates. By compiling the results of this study with those reported by O'Connor and co-workers at NETL – Albany,[85] it is now possible to determine the relative reactivity of various Ca- and Mg-bearing rocks and minerals. In evaluating materials for *ex-situ* carbon storage, the important criteria are fast reaction kinetics, relatively homogeneous mineralogy, flexibility in tuning the reaction conditions, and possible formation of high purity value-added products. In *in-situ* carbon storage, where the earth is used as a reactor system, other CO_2 immobilization mechanisms such as capillary and solubility trapping complement carbon mineralization and larger spatial scales are available for CO_2 - reaction fluid - mineral or rock interactions. Unlike *ex-situ* mineralization, where faster time scales of reactivity are preferred, in *in-situ* mineralization the time-scales of reactivity can be slower with the source rock or mineral having a smaller composition of Ca, Mg, or Fe content compared to the feedstocks for *ex-situ* mineralization. Therefore, a quantitative comparison of the reactivities of various Ca- and Mg-bearing rocks and minerals is important in this context.

Compilation of the reactivities of minerals and rocks at comparable conditions of temperature, pressure, and reaction fluid conditions shows that minerals or rocks containing abundant Ca- or Mg alumino-silicates have slower direct carbon mineralization extents compared to silicates (e.g., wollastonite, forsterite, olivine, and fayalite). Further, the reactivity of Ca-bearing minerals (wollastonite, $CaSiO_3$) is greater compared to Mg-silicates (forsterite, Mg_2SiO_4), Mg and Fe-bearing silicates (olivine $(Mg, Fe)_2SiO_4$) and iron-silicate (fayalite, Fe_2SiO_4) (**Figure 7**). The reactivity of serpentine minerals is low, except for very fine-grained, fibrous chrysotile.[95] However, the reactivity of serpentine minerals can be enhanced through heat treatment.[85,96] These data suggest that Ca- or Mg-rich silicate minerals such as wollastonite, forsterite, or

olivine, and heat-treated serpentine minerals are suitable for conversion of CO_2 to carbonates. We note, in addition, that global reserves of wollastonite are on the order of 10^8 tons,[97] whereas the mass of olivine-rich peridotite within a few km of the Earth's land surface is on the order of 10^{14} to 10^{15} tons, with an additional, even larger mass at and near the seafloor.[84] For long-term CO_2 storage, beginning with solution trapping and extending to *in situ* carbon mineralization,[98] in which reactivity is less important, basalt, gabbro and anorthosite resources are even larger than those of peridotite, and are often closer to population centers and point sources of CO_2 emissions.

Another benchmark for determining the relative reactivities of the minerals and rocks is through the comparison of the direct carbon mineralization reaction rates per unit area. However, the determination of the representative mineralization rates is complicated by the changes in the surface area as materials are converted to carbonates (**Table 3**). Moreover, while these changes in surface area are measured in some experimental studies, including ours, the average surface area of remaining reactants, products, and grains including both phases after some reaction time is not known. In this study, the mineralization rates are normalized to the average surface area of the bulk material at the beginning and the end of reaction. The experimental conditions at which the mineralization rates are determined are 185 ºC, P_{CO2} = 139 atm in 1.0 M NaCl + 0.64 M $NaHCO_3$ in 15 wt% solid for a reaction time of 3 hours.

The carbon mineralization rates of olivine, labradorite, anorthosite, and basalt at these conditions are 3.3 (+4.9 / -1.2) x 10^{-8}, 1.7 (+0.5 / -0.3) x 10^{-9}, 3.8 (+1.1 / -0.7) x 10^{-9}, and 4.8 (+0.1 / -0.1) x 10^{-10} mol m^{-2} s^{-1}, respectively (**Figure 8**). The numbers in the parentheses represent the upper and lower bounds of the reaction rates normalized to the surface area after and before the reaction. These rates show that the direct carbon mineralization rates of olivine are one to two orders of magnitude higher than that of labradorite, anorthosite, and basalt. Further, the surface areas of these materials before and after carbonation do not impact the mineralization rates by orders of magnitude. Instead, at most, changes in surface area during olivine carbonation – interpreted as equivalent to the change in the surface area of olivine grains – changes the inferred reaction rate per unit area by a factor of 2.5. These data suggest that precipitation of silica in

during the carbon mineralization of olivine is not rate limiting, while the precipitation of secondary phases and comparatively slower dissolution rates in alumino-silicate minerals can limit the extent of carbon mineralization (**Figure 9**).

5. Conclusions

The investigations reported in this study quantify the reactivities of various silicate and aluminum silicate bearing minerals and rocks such as olivine, plagioclase (labradorite), and plagioclase-rich rocks such (anorthosite and basalt). The extent of carbonation ranges from as high as 85% in olivine to as low as 9% in basalt at 185 ºC, P_{CO2} = 139 atm in aqueous fluids with 1.0 M NaCl + 0.64 M $NaHCO_3$ for a reaction time of 3 hours. The order of reactivity is: olivine > anorthosite > labradorite > basalt, as could be anticipated based on data for dissolution rates at high dilution in water with pH ~ 6 at more than 125°C as reviewed by Kelemen and co-workers.[84] The carbon mineralization behavior of plagioclase and plagioclase-bearing rocks is sensitive to temperature and $NaHCO_3$ concentration, and less sensitive to increasing the partial pressure of CO_2 from 64 to 164 atm and raising the concentration of NaCl. It is inferred from our studies and published literature that the passivation in plagioclase-rich compositions is caused by the precipitation of clay minerals and iron oxide. Significant morphological changes in the reacted minerals and rocks are also observed. Higher extents of carbonation increase the particle size and reduce the pore volume and surface area. These results suggest that a comprehensive understanding of the coupled chemical and morphological changes in magnesium and calcium silicate bearing minerals and rocks, when reacted with CO_2, is essential to predict the long-term fate of CO_2 injected into geologic reservoirs. The findings from this study also provide valuable insights into developing engineered pathways for accelerated conversion of other Ca and Mg-bearing materials (e.g., mine tailings and alkaline industrial wastes) to solid carbonates.

Author Information

Corresponding Author

***E-mail:** ap2622@columbia.edu

Notes

The authors declare no competing financial interest.

Biographies

Greeshma Gadikota is an assistant professor and Croll Sesquicentennial Fellow in the School of Civil and Environmental Engineering at Cornell University. She received her PhD in Chemical Engineering from Columbia University in 2014. Her research interests include advancing cross-scale scientific and measurements methods with a view towards developing low carbon energy and environmental technologies.

Juerg M. Matter is Associate Professor in Geoengineering within Ocean and Earth Science, National Oceanography Centre Southampton at the University of Southampton. His research interests include carbon dioxide capture and storage via in situ mineral carbonation in basalt and peridotite; monitoring and accounting techniques for carbon management; climate change mitigation; solute and reactive transport in saturated media; tracer hydrology.

Peter B. Kelemen is the Arthur D. Storke Professor in the Department of Earth and Environmental Sciences at Columbia University. His research interests include CO_2 capture and storage via in situ mineral carbonation in peridotite and basalt; melting and reactive melt transport in the Earth's mantle and lower crust; igneous processes in forming the Earth's crust; density instabilities, ductile deformation and evolution of the lower crust; subduction zone geotherms; and the mechanisms for intermediate depth earthquakes.

Patrick V. Brady_a Senior Scientist at Sandia National Laboratories. His research interests include applying geochemistry for applications related to water treatment, enhanced oil recovery, nuclear waste disposal, and climate change.

Ah-Hyung Alissa Park is the Lenfest Chair in Applied Climate Science of Earth and Environmental Engineering & Chemical Engineering at Columbia University. She is also the Director of the Lenfest Center for Sustainable Energy at the Earth Institute. Her research focuses on sustainable energy conversion pathways with emphasis on integrated carbon capture, utilization and storage (CCUS). The current efforts include the fundamental studies of chemical and physical interactions of natural and engineered materials with CO_2.

Acknowledgements

The authors would like to Frederic Enea for supporting the carbon analyses. This publication was based on work supported by U.S Department of Energy (DE-FE0002386). Peter Kelemen was also supported in part by NSF Research Grant EAR 1049905.

List of Minerals

Mineral Name	Approximate Chemical Formula
Albite	$NaAlSi_3O_8$
Anorthite	$CaAl_2Si_2O_8$
Calcic pyroxene	$(Mg,Fe)CaSi_2O_6$
Calcite	$CaCO_3$
Ca-lean pyroxenes	$(Mg,Fe)SiO_3$
Diopside	$MgCaSi_2O_6$
Enstatite	$MgSiO_3$
Fayalite	Fe_2SiO_4
Forsterite	Mg_2SiO_4
Labradorite	$(Ca,Na)(Al,Si)_4O_8$
Magnesite	$MgCO_3$
Magnetite	Fe_3O_4
Montmorillonite	$(Na, Ca)_{0.33}(Al, Mg)_2(Si_4O_{10})(OH)_2. nH_2O$
Olivine	$(Mg,Fe)_2SiO_4$
Plagioclase	$Ca_{1-x}Na_xAl_{2-x}Si_{2+x}O_8$
Sepiolite (Al-bearing)	$Mg_4Al_2Si_{10}O_{27}.15H_2O$
Serpentine	$Mg_3Si_2O_5(OH)_4$ or $(Mg,Fe)_3Si_2O_5(OH)_4$

Nomenclature

m	alkaline metal (e.g., Mg, Ca, Fe)
W_{CO2}	weight of CO_2
$W_{mineral}$	weight of mineral
R_{CO2}	mass of raw mineral/rock needed to store a unit mass of CO_2
$1/R_{CO2}$	mass of CO_2 stored in a unit mass of mineral/rock
y_m	weight fraction of alkaline metal in mineral/rock that can react with CO_2 to form carbonates
MW_m	molecular weight of alkaline metal, m
MW_{CO2}	molecular weight of CO_2 (44 g/mol)
$Y_{CO2,TCA}$	yield or extent of carbonation: mass of CO_2 stored in the mineral/rock as solid carbonate measured via Total Carbon Analysis, relative to the CO_2 storage capacity
TCA	the weight fraction of inorganic carbon in the solid sample $\left(= \left[\frac{Weight\ of\ carbon}{Weight\ of\ solid\ sample}\right]\right)$
P_{CO2}	partial pressure of CO_2 (atm)

References

(1) Gadikota, G.; Matter, J.; Kelemen, P.; Park, A.-H. A. Chemical and morphological changes during olivine carbonation for CO_2 storage in the presence of NaCl and $NaHCO_3$. *Phys. Chem. Chem. Phys.* **2014**, *16* (10), 4679–4693.

(2) Sanna, A.; Hall, M. R.; Maroto-Valer, M. Post-processing pathways in carbon capture and storage by mineral carbonation (CCSM) towards the introduction of carbon neutral materials. *Energy Environ. Sci.* **2012**, *5* (7), 7781–7796.

(3) Lackner, K. S.; Wendt, C. H.; Butt, D. P.; Joyce Jr, E. L.; Sharp, D. H. Carbon dioxide disposal in carbonate minerals. *Energy* **1995**, *20* (11), 1153–1170.

(4) Oelkers, E. H.; Gislason, S. R.; Matter, J. Mineral carbonation of CO_2. *Elements* **2008**, *4* (5), 333–337.

(5) Park, A.-H. A.; Jadhav, R.; Fan, L. CO_2 mineral sequestration : chemically enhanced aqueous carbonation of serpentine. *Can. J. Chem. Eng.* **2003**, *81*, 885–890.

(6) Park, A.-H. A.; Fan, L. S. CO_2 mineral sequestration: Physically activated dissolution of serpentine and pH swing process. *Chem. Eng. Sci.* **2004**, *59*, 5241–5247.

(7) Gerdemann, S. J.; O'Connor, W. K.; Dahlin, D. C.; Penner, L. R.; Rush, H. Ex situ aqueous mineral carbonation. *Environ. Sci. Technol.* **2007**, *41*, 2587–2593.

(8) Gadikota, G.; Park, A.-H. A. *Accelerated Carbonation of Ca- and Mg-Bearing Minerals and Industrial Wastes Using CO_2*, First edit.; Styring, P., Quadrelli, E., Armstrong, K., Eds.; Elsevier, 2014. pp 115-137.

(9) Pan, S.-Y.; Chang, E. E.; Chiang, P.-C. CO_2 capture by accelerated carbonation of alkaline wastes: a review on its principles and applications. *Aerosol Air Qual Res* **2012**, *12* (5), 770–791.

(10) Gadikota, G.; Fricker, K.; Jang, S.-H.; Park, A.-H. A. Carbonation of Silicate Minerals and Industrial Wastes and Their Potential Use as Construction Materials. In *Advances in CO_2 Capture, Sequestration, and Conversion*; Jin, F., He, L.-N., Hu, Y. H., Eds.; American Chemical Society, 2015; pp 295–322.

(11) Fricker, K. J.; Park, A.-H. A. Effect of H_2O on $Mg(OH)_2$ carbonation pathways for combined CO_2 capture and storage. *Chem. Eng. Sci.* **2013**, *100*, 332–341.

(12) Fricker, K. J.; Park, A.-H. A. Investigation of the Different Carbonate Phases and Their Formation Kinetics during $Mg(OH)_2$ Slurry Carbonation. *Ind. Eng. Chem. Res.* **2014**, *53*, 18170–18179.

(13) Swanson, E. J.; Fricker, K. J.; Sun, M.; Park, A.-H. A. Directed precipitation of hydrated and anhydrous magnesium carbonates for carbon storage. *Phys. Chem. Chem. Phys.* **2014**, *16* (42), 23440–23450.

(14) Gadikota, G.; Swanson, E. J.; Zhao, H.; Park, A.-H. A. Experimental design and data analysis for accurate estimation of reaction kinetics and conversion for carbon mineralization. *Ind. Eng. Chem. Res.* **2014**, *53* (16), 6664–6676.

(15) Gadikota, G.; Natali, C.; Boschi, C.; Park, A.-H. A. Morphological changes during enhanced carbonation of asbestos containing material and its comparison to magnesium silicate minerals. *J. Hazard. Mater.* **2014**, *264*.

(16) Zhao, H.; Park, Y.; Lee, D. H.; Park, A.-H. A. Tuning the dissolution kinetics of wollastonite via chelating agents for CO 2 sequestration with integrated synthesis of precipitated calcium carbonates. *Phys. Chem. Chem. Phys.* **2013**, *15* (36), 15185–15192.

(17) Zhao, H.; Dadap, N.; Park, A.-H. A. Tailored synthesis of precipitated magnesium carbonates as carbon-neutral filler materials during carbon mineral sequestration. **2010**, *Fluidization XIII*, 821-828.

(18) Goldberg, D.; Aston, L.; Bonneville, A.; Demirkanli, I.; Evans, C.; Fisher, A.; Garcia, H.; Gerrard, M.; Heesemann, M.; Hnottavange-Telleen, K.; et al. Geological storage of CO_2 in sub-seafloor basalt: The CarbonSAFE pre-feasibility study offshore Washington State and British Columbia. *Energy Procedia* **2018**, *146*, 158–165.

(19) Nyambura, M. G.; Mugera, G. W.; Felicia, P. L.; Gathura, N. P. Carbonation of brine impacted fractionated coal fly ash: implications for CO_2 sequestration. *J. Environ. Manage.* **2011**, *92* (3), 655–664.

(20) Montes-Hernandez, G.; Pérez-López, R.; Renard, F.; Nieto, J. M.; Charlet, L. Mineral sequestration of CO_2 by aqueous carbonation of coal combustion fly-ash. *J. Hazard. Mater.* **2009**, *161* (2–3), 1347–1354.

(21) Wang, C.; Jia, L.; Tan, Y.; Anthony, E. J. Carbonation of fly ash in oxy-fuel CFB combustion. *Fuel* **2008**, *87* (7), 1108–1114.

(22) Fauth, D. J.; Soong, Y.; White, C. M. Carbon sequestration utilizing industrial solid residues. In *Preprint Symposium*; 2002; pp 37–38.

(23) Li, X.; Bertos, M. F.; Hills, C. D.; Carey, P. J.; Simon, S. Accelerated carbonation of municipal solid waste incineration fly ashes. *Waste Manag.* **2007**, *27* (9), 1200–1206.

(24) Uliasz-Bocheńczyk, A.; Mokrzycki, E.; Piotrowski, Z.; Pomykała, R. Estimation of CO_2 sequestration potential via mineral carbonation in fly ash from lignite combustion in Poland. *Energy Procedia* **2009**, *1* (1), 4873–4879.

(25) Bauer, M.; Gassen, N.; Stanjek, H.; Peiffer, S. Carbonation of lignite fly ash at ambient T and P in a semi-dry reaction system for CO_2 sequestration. *Appl. Geochemistry* **2011**, *26* (8), 1502–1512.

(26) Larachi, F.; Gravel, J.-P.; Grandjean, B. P. A.; Beaudoin, G. Role of steam, hydrogen and pretreatment in chrysotile gas–solid carbonation: Opportunities for pre-combustion CO_2 capture. *Int. J. Greenh. Gas Control* **2012**, *6*, 69–76.

(27) Ryu, K. W.; Jang, Y. N.; Lee, M. G. Enhancement of chrysotile carbonation in alkali solution. *Mater. Trans.* **2012**, *53* (7), 1349–1352.

(28) Perez-Lopez, R.; Montes-Hernandez, G.; Nieto, J. M.; Renard, F.; Charlet, L. Carbonation of alkaline paper mill waste to reduce CO_2 greenhouse gas emissions into the atmosphere. *Appl. Geochemistry* **2008**, *23* (8), 2292–2300.

(29) Huijgen, W. J.; Witkamp, G. J.; Comans, R. N. Mineral CO_2 sequestration by steel slag carbonation. *Environ. Sci. Technol.* **2005**, *39* (24), 9676–9682.

(30) Bonenfant, D.; Kharoune, L.; Hausler, R.; Niquette, P. CO_2 Sequestration Potential of Steel Slags at Ambient Pressure and Temperature. *Ind. Eng. Chem. Res.* **2008**, *47* (20), 7610–7616.

(31) Eloneva, S.; Teir, S.; Salminen, J.; Fogelholm, C.-J.; Zevenhoven, R. Fixation of CO_2 by carbonating calcium derived from blast furnace slag. *Energy* **2008**, *33* (9), 1461–1467.

(32) Kodama, S.; Nishimoto, T.; Yamamoto, N.; Yogo, K.; Yamada, K. Development of a new pH-swing CO_2 mineralization process with a recyclable reaction solution. *Energy* **2008**, *33* (5), 776–784'.

(33) Baciocchi, R.; Costa, G.; Di Bartolomeo, E.; Polettini, A.; Pomi, R. The effects of accelerated carbonation on CO_2 uptake and metal release from incineration APC residues. *Waste Manag.* **2009**, *29* (12), 2994–3003.

(34) Chang, E. E.; Chen, C. H.; Chen, Y. H.; Pan, S. Y.; Chiang, P. C. Performance evaluation for carbonation of steel-making slags in a slurry reactor. *J. Hazard. Mater.* **2011**, *186* (1), 558–564.

(35) Chang, E. E.; Pan, S. Y.; Chen, Y. H.; Tan, C. S.; Chiang, P. C. Accelerated carbonation of steelmaking slags in a high-gravity rotating packed bed. *J. Hazard. Mater.* **2012**, *227*, 97–106.

(36) Huntzinger, D. N.; Gierke, J. S.; Sutter, L. L.; Kawatra, S. K.; Eisele, T. C. Mineral carbonation for carbon sequestration in cement kiln dust from waste piles. *J. Hazard. Mater.* **2009**, *168* (1), 31–37.

(37) Huntzinger, D. N.; Gierke, J. S.; Kawatra, S. K.; Eisele, T. C.; Sutter, L. L. Carbon dioxide sequestration in cement kiln dust through mineral carbonation. *Environ. Sci. Technol.* **2009**, *43* (6), 1986–1992.

(38) Stirling, A.; Pápai, I. H_2CO_3 Forms via HCO_3^- in Water. *J. Phys. Chem. B* **2010**, *114* (50), 16854–16859.

(39) Wang, X.; Conway, W.; Burns, R.; McCann, N.; Maeder, M. Comprehensive Study of the Hydration and Dehydration Reactions of Carbon Dioxide in Aqueous Solution. *J. Phys. Chem. A* **2009**, *114* (4), 1734–1740.

(40) Awad, A.; van Groos, A.; Guggenheim, S. Forsteritic olivine : Effect of crystallographic direction on dissolution kinetics. *Geochim. Cosmochim. Acta* **2000**, *64* (10), 1765–1772.

(41) Rosso, J. J.; Rimstidt, D. J. A high resolution study of forsterite dissolution rates. *Geochim. Cosmochim. Acta* **2000**, *64* (5), 797–811.

(42) Chen, Y.; Brantley, S. L. Dissolution of forsteritic olivine at 65 °C and $2 < pH < 5$. *Chem. Geol.* **2000**, *165*, 267–281.

(43) Giammar, D. E.; Bruant, R. G.; Peters, C. A. Forsterite dissolution and magnesite precipitation at conditions relevant for deep saline aquifer storage and sequestration of carbon dioxide. *Chem. Geol.* **2005**, *217* (3–4), 257–276.

(44) Oelkers, E. H. An experimental study of forsterite dissolution rates as a function of temperature and aqueous Mg and Si concentrations. *Chem. Geol.* **2000**, *175*, 485–494.

(45) Pokrovsky, O.; Schott, J. Kinetics and mechanism of forsterite dissolution at 25 °C and pH from 1 to 12. *Geochim. Cosmochim. Acta* **2000**, *64* (19), 3313–3325.

(46) Wogelius, R. A.; Walther, J. V. Olivine dissolution kinetics at near-surface conditions. *Chem. Geol.* **1992**, *97* (1–2), 101–112.

(47) Hänchen, M.; Prigiobbe, V.; Storti, G.; Seward, T. M.; Mazzotti, M. Dissolution kinetics of fosteritic olivine at 90–150 °C including effects of the presence of CO_2. *Geochim. Cosmochim. Acta* **2006**, *70* (17), 4403–4416.

(48) Prigiobbe, V.; Costa, G.; Baciocchi, R.; Hänchen, M.; Mazzotti, M. The effect of CO_2 and salinity on olivine dissolution kinetics at. *Chem. Eng. Sci.* **2009**, *64* (15), 3510–3515.

(49) Carroll, S. A.; Knauss, K. G. Dependence of labradorite dissolution kinetics on $CO_{2(aq)}$, $Al_{(aq)}$, and temperature. *Chem. Geol.* **2005**, *217* (3–4), 213–225.

(50) Cygan, R. T.; Casey, W. H.; Boslough, M. B.; Westrich, H. R.; Carr, M. J.; Holdren, G. R. Dissolution kinetics of experimentally shocked silicate minerals. *Chem. Geol.* **1989**, *78* (3–4), 229–244.

(51) Siegel, D. I.; Pfannkuch, H. O. Silicate mineral dissolution at pH 4 and near standard temperature and pressure. *Geochim. Cosmochim. Acta* **1984**, *48* (1), 197–201.

(52) van Hees, P. A. W.; Lundstro, U. S.; Morth, C. M. Dissolution of microcline and labradorite in a forest O horizon extract : the effect of naturally occurring organic acids. **2002**, *189*, 199–211.

(53) Amrhein, C.; Suarez, D. L. Some factors affecting the dissolution kinetics of anorthite at 25 °C. *Geochim. Cosmochim. Acta* **1992**, *56* (5), 1815–1826.

(54) Oelkers, E. H.; Schott, J. Experimental study of anorthite dissolution and the relative mechanism of feldspar hydrolysis. *Geochim. Cosmochim. Acta* **1995**, *59* (24), 5039–5053.

(55) Gislason, S. R.; Oelkers, E. H. Mechanism, rates, and consequences of basaltic glass dissolution: II. An experimental study of the dissolution rates of basaltic glass as a function of pH and temperature. *Geochim. Cosmochim. Acta* **2003**, *67* (20), 3817–3832.

(56) Gudbrandsson, S.; Wolff-Boenisch, D.; Gislason, S. R.; Oelkers, E. H. An experimental study of crystalline basalt dissolution from 2<=pH<=11 and temperatures from 5 to 75°C. *Geochim. Cosmochim. Acta* **2011**, *75* (19), 5496–5509.

(57) Guy, C.; Schott, J. Multisite surface reaction versus transport control during the hydrolysis of a complex oxide. *Chem. Geol.* **1989**, *78* (3–4), 181–204.

(58) Oelkers, E. H.; Gislason, S. R. The mechanism, rates and consequences of basaltic glass dissolution: I. An experimental study of the dissolution rates of basaltic glass as a function of aqueous Al, Si and oxalic acid concentration at 25°C and pH 3 and 11. *Geochim. Cosmochim. Acta* **2001**, *65* (21), 3671–3681.

(59) Schaef, H. T.; McGrail, B. P. Dissolution of Columbia River Basalt under mildly acidic conditions as a function of temperature: Experimental results relevant to the geological sequestration of carbon dioxide. *Appl. Geochemistry* **2009**, *24* (5), 980–987.

(60) Wolff-Boenisch, D.; Wenau, S.; Gislason, S. R.; Oelkers, E. H. Dissolution of basalts and peridotite in seawater, in the presence of ligands, and CO_2: Implications for mineral sequestration of carbon dioxide. *Geochim. Cosmochim. Acta* **2011**, *75* (19), 5510–5525.

(61) Wolff-Boenisch, D.; Gislason, S. R.; Oelkers, E. H. The effect of crystallinity on dissolution rates and CO2 consumption capacity of silicates. *Geochim. Cosmochim. Acta* **2006**, *70* (4), 858–870.

(62) Wolff-Boenisch, D.; Gislason, S. R.; Oelkers, E. H.; Putnis, C. V. The dissolution rates of natural glasses as a function of their composition at pH 4 and 10.6, and temperatures from 25 to 74 °C. *Geochim. Cosmochim. Acta* **2004**, *68* (23), 4843–4858.

(63) Hänchen, M.; Prigiobbe, V.; Baciocchi, R.; Mazzotti, M. Precipitation in the Mg-carbonate system—effects of temperature and CO_2 pressure. *Chem. Eng. Sci.* **2008**, *63* (4), 1012–1028.

(64) Saldi, G. D.; Jordan, G.; Schott, J.; Oelkers, E. H. Magnesite growth rates as a function of temperature and saturation state. *Geochim. Cosmochim. Acta* **2009**, *73* (19), 5646–5657.

(65) Saldi, G. D.; Schott, J.; Pokrovsky, O. S.; Gautier, Q.; Oelkers, E. H. An experimental study of magnesite precipitation rates at neutral to alkaline conditions and 100–200 °C as a function of pH, aqueous solution composition and chemical affinity. *Geochim. Cosmochim. Acta* **2012**, *83*, 93–109.

(66) O'Connor, W. K.; Dahlin, D. C.; Nilsen, D. N.; Walters, R. P.; Turner, P. C. *Carbon dioxide sequestration by direct mineral carbonation with carbonic acid (No. DOE/ARC-2000-008)*; 2000.

(67) O'Connor, W. K.; Dahlin, D. C.; Rush, G. E.; Gerdemann, S. J.; Nilsen, D. N. *Final report: Aqueous mineral carbonation: DOE/ARC-TR-04-002*; 2004.

(68) Rush, G. E.; Connor, W. K. O.; Dahlin, D. C.; Penner, L. R.; Gerdemann, S. J. *Laboratory Tests of Mafic , Ultra-Mafic , and Sedimentary Rock Types for In-Situ Applications for Carbon Dioxide Sequestration: DOE/ARC-2004-038*; 2004.

(69) Schaef, H. T.; McGrail, B. P.; Owen, A. T.; Arey, B. W. Mineralization of basalts in the CO_2 – H_2O – H_2S system. *Int. J. Greenh. Gas Control* **2013**, *16*, 187–196.

(70) Schaef, H. T.; McGrail, B. P.; Owen, A. T. Basalt- CO_2–H_2O interactions and variability in carbonate mineralization rates. *Energy Procedia* **2009**, *1* (1), 4899–4906.

(71) Matter, J. M.; Broecker, W. S.; Stute, M.; Gislason, S. R.; Oelkers, E. H.; Stefánsson, A.; Wolff-Boenisch, D., Gunnlaugsson, E., Axelsson, G.; Björnsson, G. Permanent carbon dioxide storage into basalt: the CarbFix pilot project, Iceland. *Energy Procedia* **2009**, *1* (1), 3641–3646.

(72) Béarat, H.; McKelvy, M. J.; Chizmeshya, A.V., Gormley, D.; Nunez, R.; Carpenter, R. W.; Squires, K.; Wolf, G. H. Carbon sequestration via aqueous olivine mineral carbonation: role of passivating layer formation. *Environ. Sci. Technol.* **2006**, *40* (15), 4802–4808.

(73) King, H. E.; Plümper, O.; Putnis, A. Effect of secondary phase formation on the carbonation of olivine. *Environ. Sci. Technol.* **2010**, *44* (16), 6503–6509.

(74) Saldi, G. D.; Daval, D.; Morvan, G.; Knauss, K. G. The role of Fe and redox conditions in olivine carbonation rates: An experimental study of the rate limiting reactions at 90 and 150°C in open and closed systems. *Geochim. Cosmochim. Acta* **2013**, *118*, 157–183.

(75) Munz, I. A.; Brandvoll, Ø.; Haug, T. A.; Iden, K.; Smeets, R.; Kihle, J.; Johansen, H. Mechanisms and rates of plagioclase carbonation reactions. *Geochim. Cosmochim. Acta* **2012**, *77*, 27–51.

(76) Hellevang, H.; Haile, B. G.; Tetteh, A. Experimental study to better understand factors affecting the CO_2 mineral trapping potential of basalt. *Greenh. Gases Sci. Technol.* **2017**, *7*, 143–157.

(77) Chizmeshya, A. V. G.; McKelvy, M. J.; Squires, K.; Carpenter, R. W.; Béarat, H. *A novel approach to mineral carbonation: Enhancing carbonation while avoiding mineral pretreatment process cost: DOE Final Report 924162*; 2007.

(78) Hövelmann, J.; Putnis, C. V.; Ruiz-Agudo, E.; Austrheim, H. Direct nanoscale observations of CO_2 sequestration during brucite [Mg(OH)2] dissolution. *Environ. Sci. Technol.* **2012**, *46* (9), 5253–5260.

(79) Brady, P. V; Dorn, R. I.; Brazel, A. J.; Clark, J.; Moore, R. B.; Glidewell, T. Direct measurement of the combined effects of lichen, rainfall, and temperature on silicate weathering. *Geochim. Cosmochim. Acta* **1999**, *63* (19), 3293–3300.

(80) Bénézeth, P.; Saldi, G. D.; Dandurand, J.-L.; Schott, J. Experimental determination of the solubility product of magnesite at 50 to 200 °C. *Chem. Geol.* **2011**, *286* (1–2), 21–31.

(81) He, S.; Morse, J. W. The carbonic acid system and calcite solubility in aqueous Na-K-Ca-Mg-Cl-SO4 solutions from 0 to 90 °C. *Geochim. Cosmochim. Acta* **1993**, *57* (15), 3533–3554.

(82) Ellis, A. J. The solubility of calcite in sodium chloride solutions at high temperatures. *Am. J. Sci.* **1963**, *261* (3), 259–267.

(83) Eikeland, E.; Blichfeld, A. B.; Tyrsted, C.; Jensen, A.; Iversen, B. B. Optimized carbonation of magnesium silicate mineral for CO_2 storage. *ACS Appl. Mater. Interfaces* **2015**, *7* (9), 5258–5264.

(84) Kelemen, P. B.; Matter, J.; Streit, E. E.; Rudge, J. F.; Curry, W. B.; Blusztajn, J. Rates and Mechanisms of Mineral Carbonation in Peridotite: Natural Processes and Recipes for Enhanced, in situ CO_2 Capture and Storage. *Annu. Rev. Earth Planet. Sci.* **2011**, *39* (1), 545–576.

(85) O'Connor, W. K.; Rush, G. E.; Dahlin, D. C.; Reidel, S. P.; Johnson, V. G. Geological Sequestration of CO_2 in the Columbia River Basalt Group. In *28th International Technical Conference on Coal Utilization & Fuel Systems*; Clearwater, Florida, 2003.

(86) Eggleston, C. M.; Hochella Jr, M. F.; Parks, G. A. Sample preparation and aging effects on the dissolution rate and surface composition of diopside. *Geochim. Cosmochim. Acta* **1989**, *53*, 797–804.

(87) Hangx, S. J. T.; Spiers, C. J. Reaction of plagioclase feldspars with CO_2 under hydrothermal conditions. *Chem. Geol.* **2009**, *265* (1–2), 88–98.

(88) Palandri, J. L.; Kharaka, Y. K. *A compilation of rate parameters of water-mineral interaction kinetics for application to geochemical modeling: Open File Report 2004-1068*; 2004.

(89) Weyl, P. . The change in solubility of calcium carbonate with temperature and carbon dioxide content. *Geochim. Cosmochim. Acta* **1959**, *17* (3–4), 214–225.

(90) Parkhurst, D. L.; Appelo, C. A. J. *User's guide to PHREEQC (Version 2). Water Resources Investigations Report: 99–4259*; 1999.

(91) Duan, Z.; Sun, R.; Zhu, C.; Chou, I. M. An improved model for the calculation of CO_2 solubility in aqueous solutions containing Na^+, K^+, Ca^{2+}, Mg^{2+}, Cl^-, and SO_4^{2-}. *Mar. Chem.* **2006**, *98* (2–4), 131–139.

(92) Olsen, A. A. *Forsterite dissolution kinetics: Applications and implications for chemical weathering [PhD thesis]*; Blacksburg VA, USA, 2007.

(93) King, H. E.; Plümper, O.; Putnis, A. Effect of secondary phase formation on the carbonation of olivine. *Environ. Sci. Technol.* **2010**, *44* (16), 6503–6509.

(94) Saldi, G. D.; Daval, D.; Morvan, G.; Knauss, K. G. The role of Fe and redox conditions in olivine carbonation rates: an experimental study of the rate limiting reactions at 90 and 150 °C in open and closed systems. *Geochim. Cosmochim. Acta* **2013**, *118*, 157–183.

(95) Thom, J. G. M.; Dipple, G. M.; Power, I. M.; Harrison, A. L. Chrysotile dissolution rates: Implications for carbon sequestration. *Appl. Geochemistry* **2013**, *35*, 244–254.

(96) Pasquier, L.-C.; Mercier, G.; Blais, J.-F.; Cecchi, E.; Kentish, S. Reaction mechanism for the aqueous-phase mineral carbonation of heat-activated serpentine at low temperatures and pressures in flue gas conditions. *Environ. Sci. Technol.* **2014**, *48* (9), 5163–5170.

(97) USGS. *Wollastonite, Mineral Commodity Summaries*; 2018.

(98) Matter, J. M.; Stute, M.; Snæbjörnsdottir, S. Ó.; Oelkers, E. H.; Gislason, S. R.; Aradottir, E. S.; Sigfusson, B.; Gunnarsson, I.; Sigurdardottir, H.; Gunnlaugsson, E.; et al. Rapid carbon mineralization for permanent disposal of anthropogenic carbon dioxide emissions. *Science.* **2016**, *352* (6291), 1312–1314.

Table 1. Compositions of labradorite, anorthosite and basalt used in this study. Olivine composition noted in this table is based on the data reported in [1]

Analyte	Labradorite (wt%)	Anorthosite (wt%)	Basalt (wt%)	Olivine (wt%)
CaO	10.20	14.10	8.15	0.16
MgO	0.24	8.74	4.82	47.30
Fe_2O_3	0.97	10.60	14.60	13.90
SiO_2	54.30	41.80	51.90	39.70
Al_2O_3	28.00	24.20	13.40	0.20
Na_2O	5.05	0.59	2.91	0.01
K_2O	0.59	0.03	1.09	<0.01
TiO_2	0.14	0.04	1.74	<0.01
P_2O_5	0.04	<0.01	0.32	<0.01
MnO	0.01	0.13	0.21	0.15
Cr_2O_3	0.10	0.08	0.10	0.78
V_2O_5	<0.01	<0.01	0.06	<0.01
LOI*	0.32	0.12	0.27	-0.70
Carbonation Potential, $\frac{W_{CO_{2,max}}}{W_{mineral}}$ (assuming that Fe does not react to form $FeCO_3$)	0.105	0.171	0.076	0.343
Carbonation Potential, $\frac{W_{CO_{2,max}}}{W_{mineral}}$ (assuming that Fe reacts to form $FeCO_3$)	0.206	0.157	0.081	0.374
Mg#[1]	-	66	49	87
An#[2]	53	98	61	-

*LOI: Loss of Ignition; Material is heated to 1000 °C until there is no change in the weight of the sample.

[1] $Mg\# = molar\ \frac{Mg}{Mg+Fe}$; [2] $An\# = molar\ \frac{Ca}{Ca+Na}$; Mg# and An# are molar ratios that represent relative abundances of elements in mineral solid solutions.

Table 2. Summary of the extents of carbonation of olivine, labradorite, anorthosite and basalt reacted at varying reaction times, temperatures, and CO_2 partial pressures, and in the presence of various chemical additives. The solid (mineral/rock) to liquid ratio was 15 wt% and a stirring speed of 800 rpm was maintained. Extents of carbonation are reported as an average of TCA estimates for labradorite, anorthosite and basalt, and as an average of both TCA and TGA for olivine. (Reported values are the average and standard deviation (1 sigma) for three runs of Total Carbon Analysis (TCA))

	Extent of Carbonation (%)			
	Labradorite	Anorthosite	Basalt	Olivine
Effect of Reaction Time *(185 °C, P_{CO2} =139 atm, 1.0 M NaCl+0.64 M $NaHCO_3$)*				
1 hour	10.8 ± 0.6	6.6 ± 0.5	8.4 ± 0.6	56.6 ± 1.5
3 hours	35.3 ± 0.4	19.4 ± 0.5	8.6 ± 0.1	85.3 ± 3.1
5 hours	46.0 ± 0.1	20.1 ± 0.4	9.9 ± 0.6	90.5 ± 5.6
Effect of Partial Pressure of CO_2 *(185 °C, 3 hours, 1.0 M NaCl+0.64 M $NaHCO_3$)*				
64 atm	33.8 ± 0.4	18.4 ± 0.2	8.2 ± 0.3	39.3 ± 0.9
89 atm	34.9 ± 1.0	19.1 ± 0.6	8.1 ± 0.2	59.9 ± 2.1
139 atm	35.3 ± 0.4	19.8 ± 0.5	8.6 ± 0.1	85.3 ± 3.1
164 atm	38.6 ± 0.8	18.9 ± 0.2	9.6 ± 0.8	83.9 ± 2.8
Effect of Temperature *(P_{CO2} = 139 atm, 3 hours, 1.0 M NaCl+0.64 M $NaHCO_3$)*				
90 °C	13.9 ± 0.3	5.9 ± 0.3	5.5 ± 0.2	3.0 ± 0.3
125 °C	14.1 ± 0.1	6.9 ± 0.3	7.1 ± 0.3	28.2 ± 0.4
150 °C	25.6 ± 0.2	10.3 ± 0.4	7.7 ± 0.3	70.5 ± 1.8
185 °C	35.3 ± 0.4	19.3 ± 0.5	8.6 ± 0.1	85.3 ± 3.1
Effect of [$NaHCO_3$] *(185 °C, P_{CO2} = 139 atm, 3 hours)*				
Deionized Water	4.8 ± 0.2	7.7 ± 0.1	3.5 ± 0.3	5.8 ± 0.3
0.48 M $NaHCO_3$	8.4 ± 0.1	8.2 ± 0.3	7.8 ± 0.4	56.0 ± 0.5
0.64 M $NaHCO_3$	11.6 ± 0.4	10.4 ± 0.4	10.4 ± 0.0	82.7 ± 3.6
1.0 M $NaHCO_3$	33.8 ± 0.7	25.8 ± 0.1	14.5 ± 0.6	85.0 ± 1.9
Effect of [NaCl] *(185 °C, P_{CO2} = 139 atm, 3 hours)*				
Deionized Water	4.8 ± 0.2	7.7 ± 0.1	3.5 ± 0.3	5.8 ± 0.3
0.5 M NaCl	3.9 ± 0.7	7.2 ± 0.2	4.2 ± 0.1	6.8 ± 0.3
1.0 M NaCl	3.4 ± 0.4	8.5 ± 0.5	5.7 ± 0.1	14.4 ± 0.9

Table 3. Changes in the mean particle diameter and specific surface area of olivine, labradorite, anorthosite and basalt due to carbonation reaction. Experiments were conducted at 185 ^{o}C and P_{CO2} = 139 atm in 1.0 M NaCl + 0.64 M $NaHCO_3$ for 3 hours, with 15 wt% slurry concentration and a stirring speed of 800 rpm. Olivine data shown in this table is based on measurements reported by Gadikota et al.[1]

Materials	Mean Particle Diameter ± Standard Deviation (μm)	Surface Area ± Standard Deviation (m^2/g)
Olivine	21.41 ± 0.23	3.77 ± 0.17
Carbonated Olivine	27.34 ± 0.31	0.96 ± 0.29
Labradorite	8.20 ± 0.21	4.46 ± 0.01
Carbonated Labradorite	10.23 ± 0.33	2.74 ± 0.35
Anorthosite	9.68 ± 0.17	2.92 ± 0.05
Carbonated Anorthosite	12.07 ± 0.26	1.82 ± 0.16
Basalt	7.46 ± 0.08	4.48 ± 0.09
Carbonated Basalt	9.36 ± 0.07	4.32 ± 0.40

Captions for figures

Figure 1. Effect of reaction time on (a) the extent of carbonation of labradorite, anorthosite, and basalt. Experiments were conducted at 185 ºC, P_{CO2} = 139 atm in 1.0 M NaCl + 0.64 M $NaHCO_3$ with slurry concentration of 15 wt% and a stirring speed of 800 rpm. The conversion of (b) olivine and (c) labradorite are compared to literature values as well as the exhaustion model predictions.

Figure 2. (a) Effect of CO_2 partial pressure on the extent of carbonation of labradorite, anorthosite, and basalt as well as previously reported olivine [1]. Experiments performed at 185 ºC in 1.0 M NaCl + 0.64 M $NaHCO_3$ for 3 hours, with slurry density of 15 wt% and a stirring speed of 800 rpm. (b) Relationship between the partial pressure of CO_2 and CO_2 density with the extent of olivine carbonation.

Figure 3. Effect of temperature on the extent of carbonation of labradorite, anorthosite and basalt compared to previously reported olivine carbonation data [1]. Experiments performed at P_{CO2} = 139 atm in 1.0 M NaCl + 0.64 M $NaHCO_3$ for 3 hours, with slurry density of 15 wt% and a stirring speed of 800 rpm.

Figure 4. Effect of (a) $NaHCO_3$ and (b) NaCl on the extent of carbonation of labradorite, anorthosite, and basalt compared to previously reported olivine carbonation data [1]. Experiments performed at 185 ºC, P_{CO2} = 139 atm for 3 hours, with slurry density of 15 wt% and a stirring speed of 800 rpm.

Figure 5. Changes in the cumulative pore volume of (a) olivine, (b) labradorite, (c) anorthosite, and (d) basalt when reacted with CO_2 at 185 ºC, P_{CO2} = 139 atm in 1.0 M NaCl + 0.64 M $NaHCO_3$ for 3 hours, with slurry density of 15 wt% and a stirring speed of 800 rpm. Olivine pore volume data was previously reported by Gadikota and co-workers [1] and plotted here for comparison.

Figure 6. SEM images showing the formation of (a) magnesite in olivine, (b) calcite in labradorite, (c) magnesite and calcite in anorthosite, and (d) magnesite and calcite in basalt. Carbonation experiments performed at 185 ºC, P_{CO2} = 139 atm in 1.0 M NaCl + 0.64 M $NaHCO_3$ for 3 hours, with slurry density of 15 wt% and a stirring speed of 800 rpm. Reacted olivine shown here for comparison is based on the carbon mineralization studies reported by Gadikota et al. [1].

Figure 7. Comparison of the reactivities of various Ca and Mg-bearing minerals and rocks and their CO_2 storage potential. These comprehensive data are from this study (grey colored minerals/rocks), olivine data reported by Gadikota et al. [1] and other data reported by O' Connor and co-workers at NETL-Albany [85]. The experiments at NETL-Albany were performed at 185 ºC and P_{CO2} = 150 atm in 1.0 M NaCl + 0.64 M $NaHCO_3$, 15 wt% slurry concentration and a stirring rate of 1000 rpm. Our experiments were also performed under very similar reaction conditions (185 ºC, P_{CO2} = 139 atm in 1.0 M NaCl + 0.64 M $NaHCO_3$, 15 wt% slurry concentration and a stirring rate of 800 rpm).

Figure 8. Comparison of the direct carbon mineralization rates of olivine, labradorite, anorthosite, and basalt normalized to the surface area before and after the reaction (see Table 4) as represented by the upper and lower limit bars. The rates reported here represent experiments performed at 185 ºC and P_{CO2} = 139 atm in 1.0 M NaCl + 0.64 M $NaHCO_3$ for 3 hours, with 15 wt% slurry

concentration and a stirring speed of 800 rpm. Rate data for olivine is based on the extent of carbon mineralization reported by Gadikota et al. [1] and plotted here for comparison.

Figure 9. Schematic representation of carbon mineralization with (a) anorthite, $CaAl_2Si_2O_8$ and (b) forsterite, Mg_2SiO_4 at similar experimental conditions of 185 ^oC, P_{CO2} = 139 atm in 1.0 M NaCl + 0.64 M $NaHCO_3$ in 15 wt% solid for a reaction time of 3 hours.

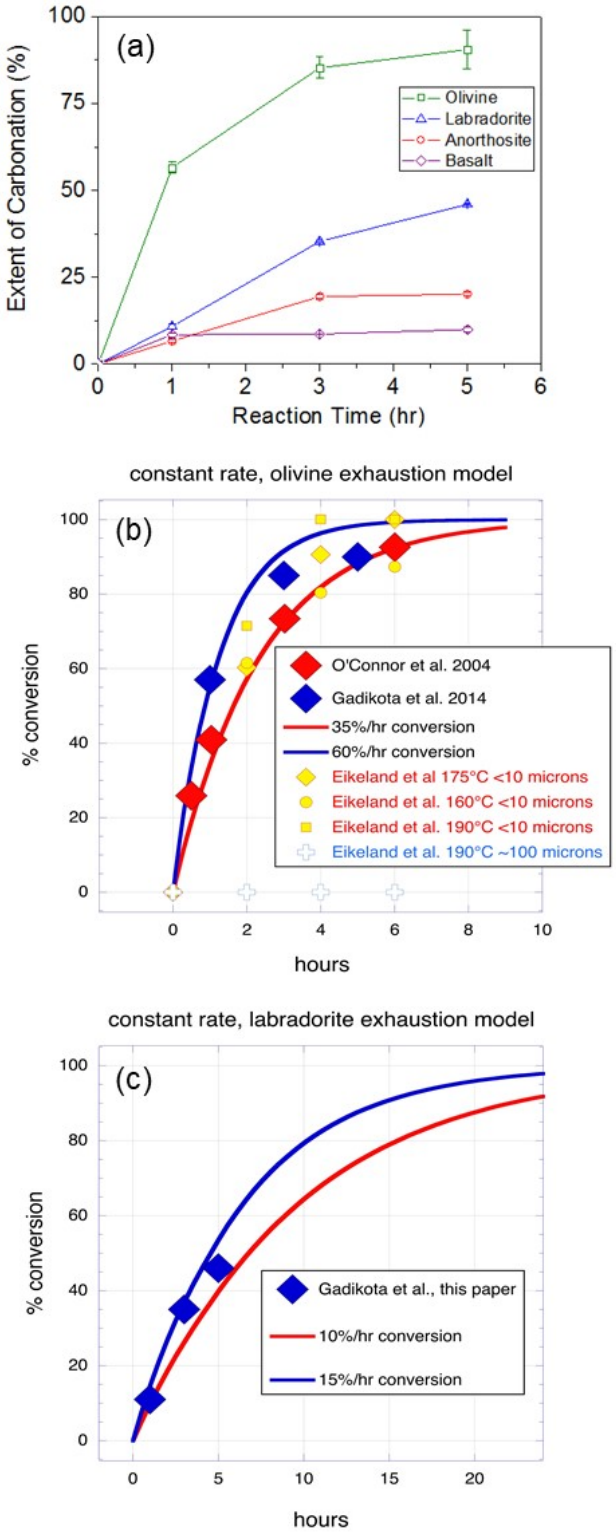

Figure 1. Effect of reaction time on (a) the extent of carbonation of labradorite, anorthosite, and basalt. Experiments were conducted at 185 °C, P_{CO2} = 139 atm in 1.0 M NaCl + 0.64 M $NaHCO_3$ with slurry concentration of 15 wt% and a stirring speed of 800 rpm. The conversion of (b) olivine and (c) labradorite are compared to literature values as well as the exhaustion model predictions.

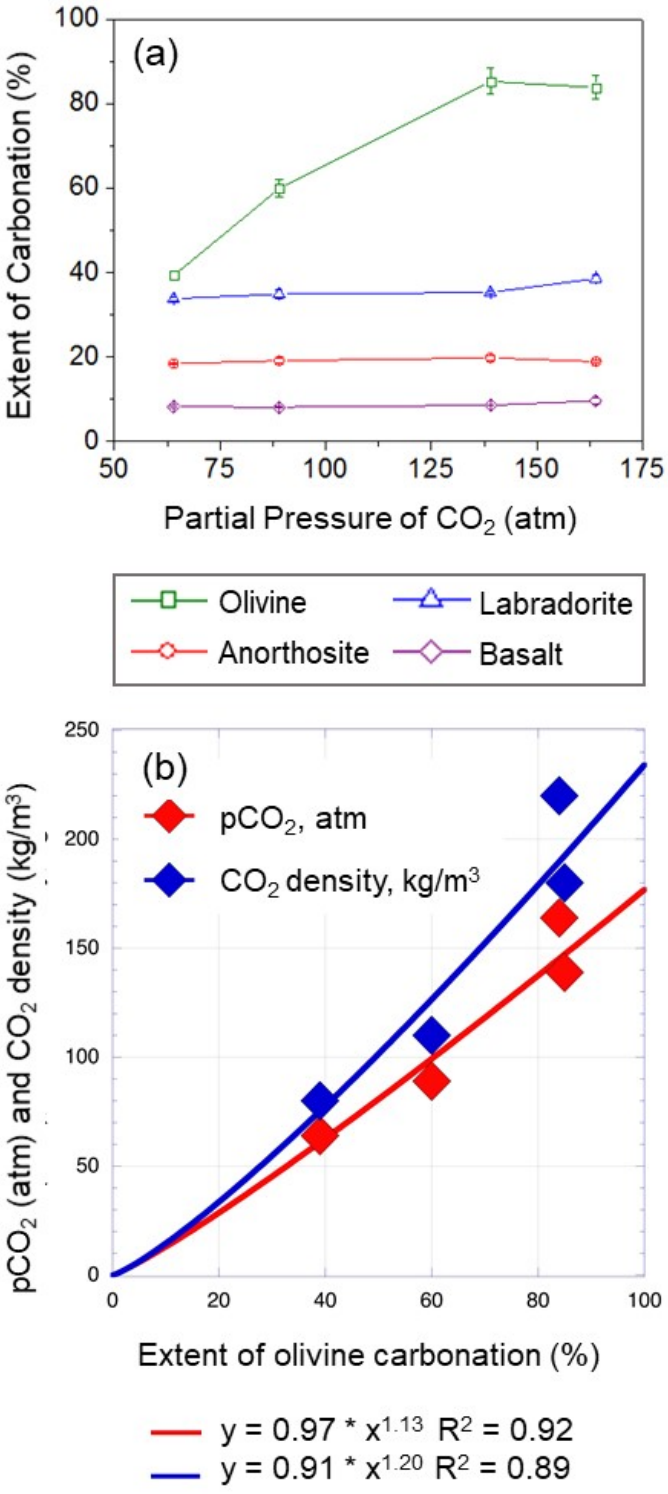

Figure 2. (a) Effect of CO_2 partial pressure on the extent of carbonation of labradorite, anorthosite, and basalt as well as previously reported olivine [1]. Experiments performed at 185 °C in 1.0 M NaCl + 0.64 M $NaHCO_3$ for 3 hours, with slurry density of 15 wt% and a stirring speed of 800 rpm. (b) Relationship between the partial pressure of CO_2 and CO_2 density with the extent of olivine carbonation.

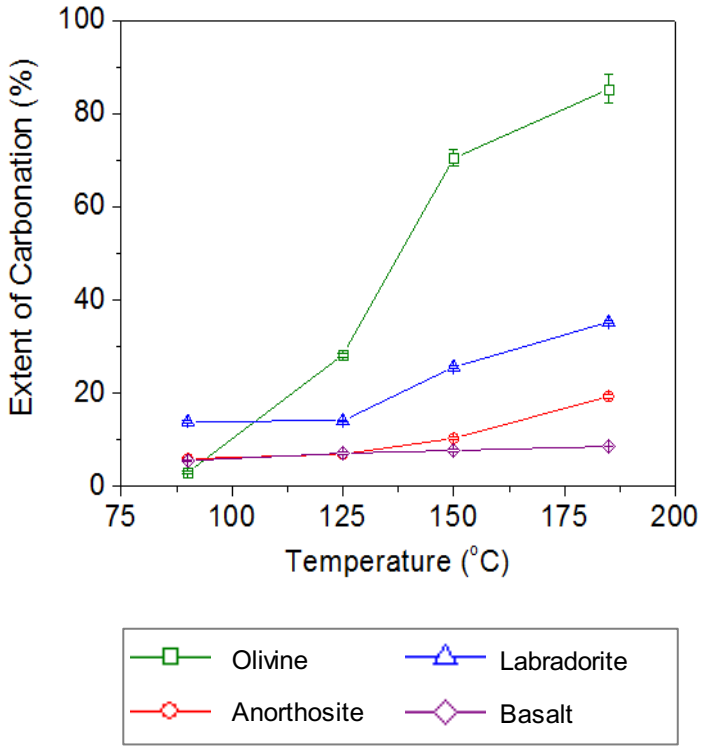

Figure 3. Effect of temperature on the extent of carbonation of labradorite, anorthosite and basalt compared to previously reported olivine carbonation data [1]. Experiments performed at P_{CO2} = 139 atm in 1.0 M NaCl + 0.64 M $NaHCO_3$ for 3 hours, with slurry density of 15 wt% and a stirring speed of 800 rpm.

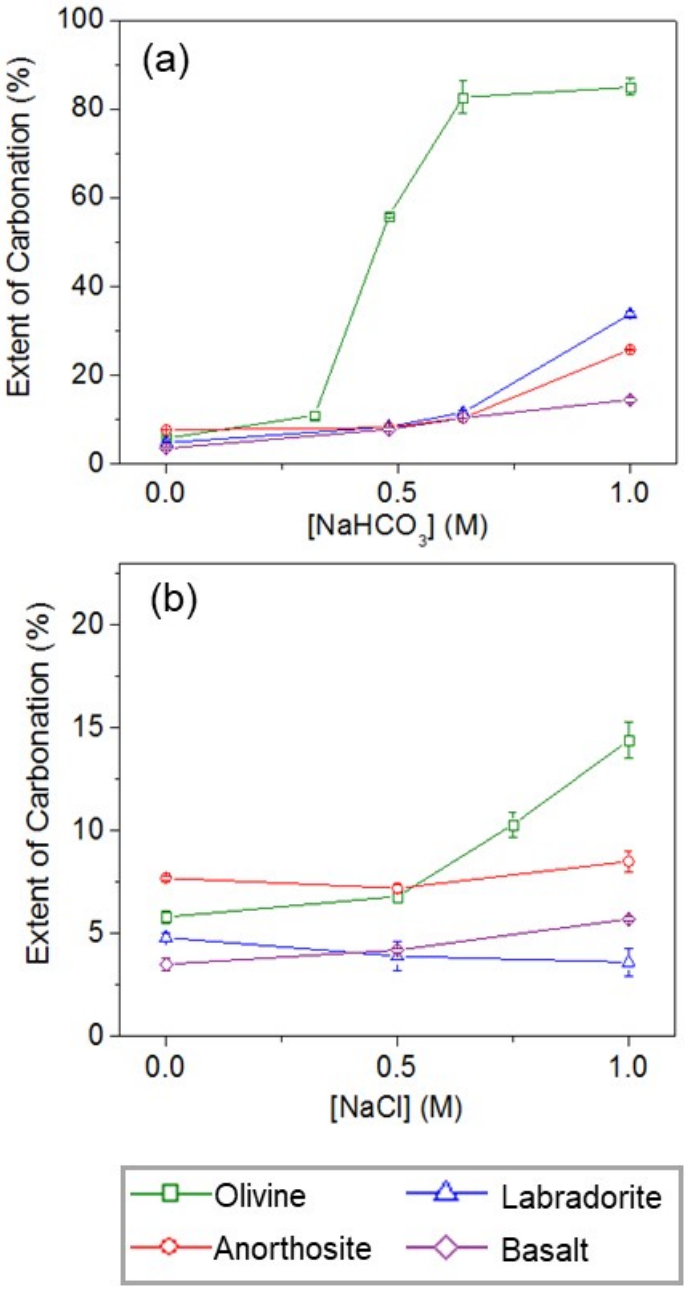

Figure 4. Effect of (a) $NaHCO_3$ and (b) NaCl on the extent of carbonation of labradorite, anorthosite, and basalt compared to previously reported olivine carbonation data [1]. Experiments performed at 185 °C, P_{CO2} = 139 atm for 3 hours, with slurry density of 15 wt% and a stirring speed of 800 rpm.

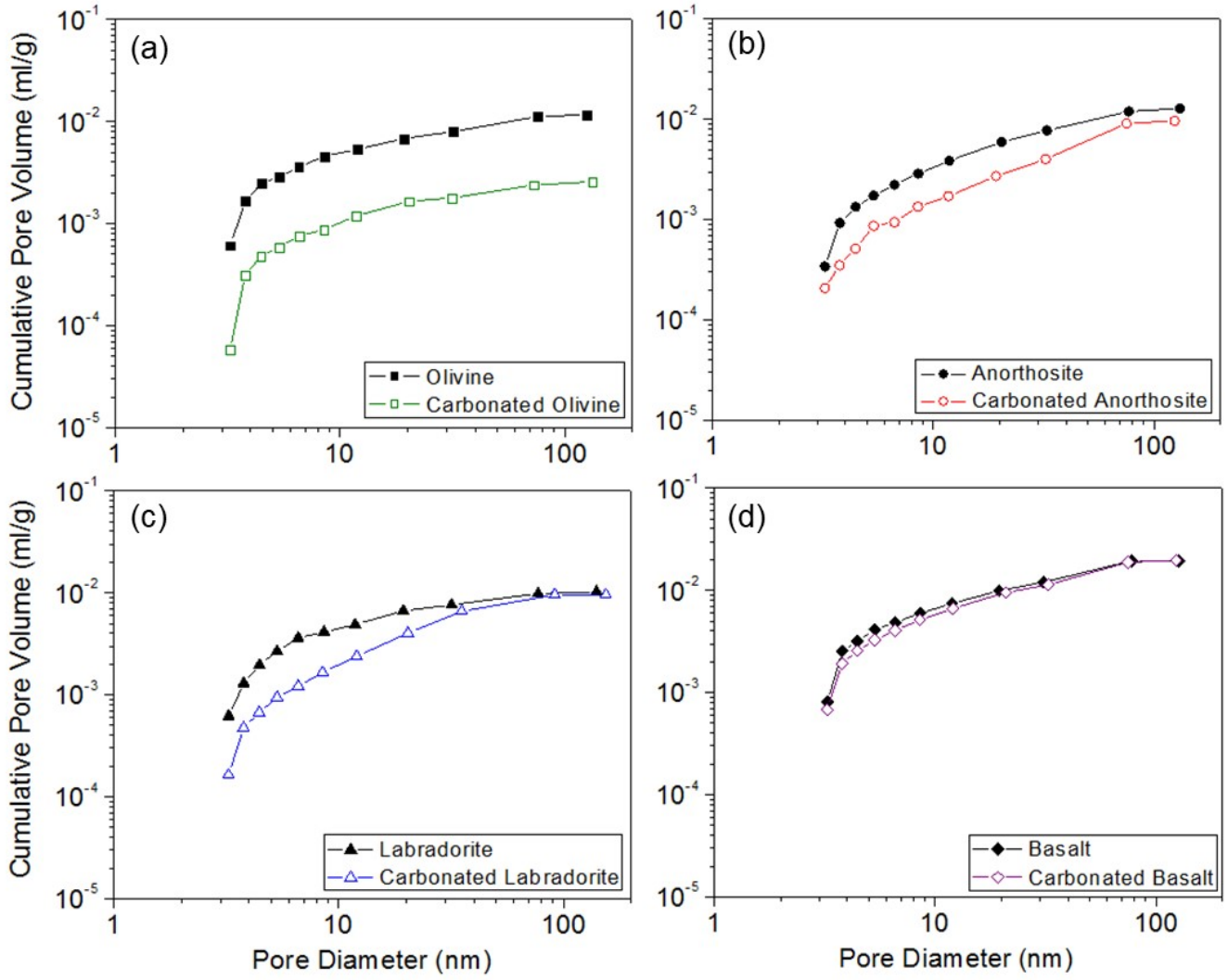

Figure 5. Changes in the cumulative pore volume of (a) olivine, (b) anorthosite, (c) labradorite, and (d) basalt when reacted with CO_2 at 185 °C, P_{CO2} = 139 atm in 1.0 M NaCl + 0.64 M $NaHCO_3$ for 3 hours, with slurry density of 15 wt% and a stirring speed of 800 rpm. Olivine pore volume data was previously reported by Gadikota and co-workers [1] and plotted here for comparison.

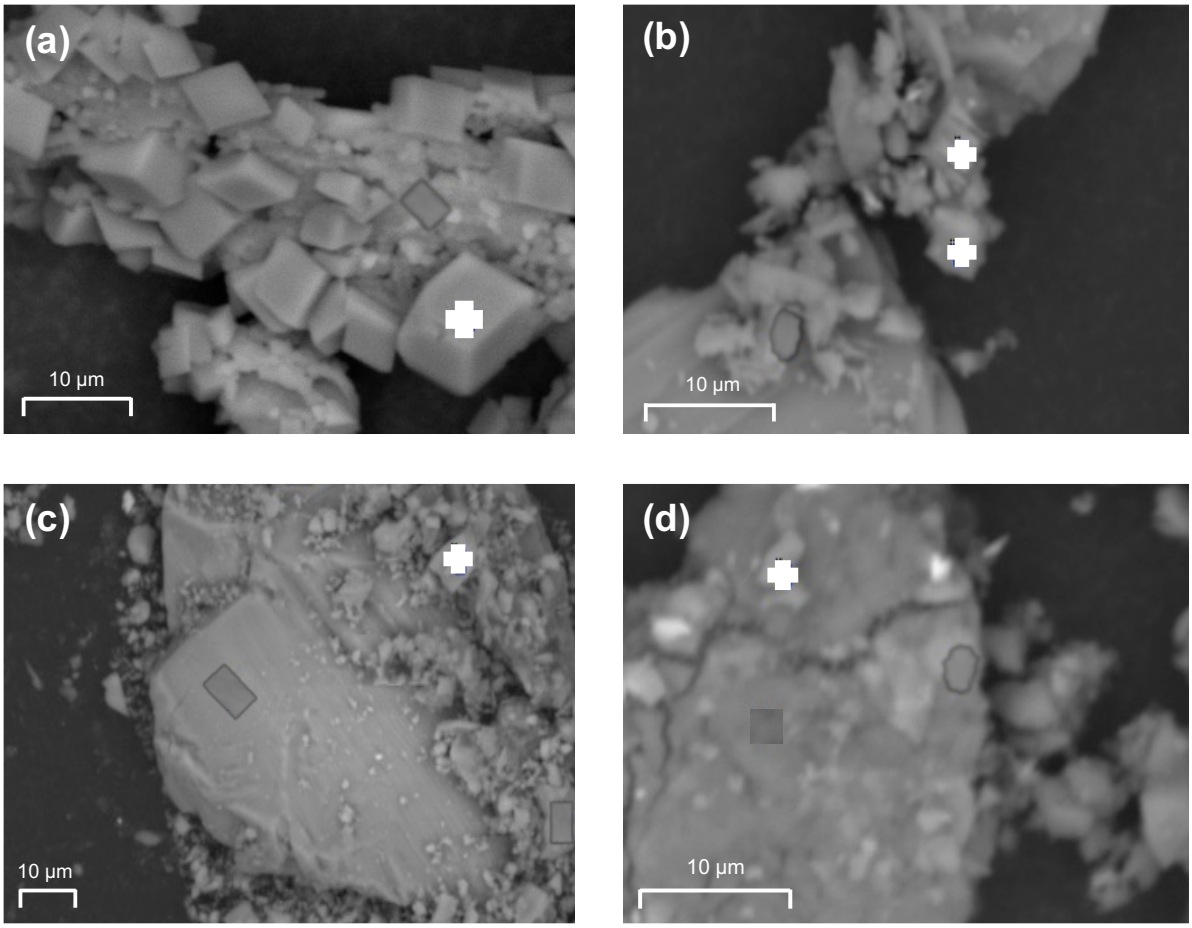

Figure 6. SEM images showing the formation of (a) magnesite in olivine, (b) calcite in labradorite, (c) magnesite and calcite in anorthosite, and (d) magnesite and calcite in basalt. Carbonation experiments performed at 185 °C, P_{CO2} = 139 atm in 1.0 M NaCl + 0.64 M $NaHCO_3$ for 3 hours, with slurry density of 15 wt% and a stirring speed of 800 rpm. Reacted olivine shown here for comparison is based on the carbon mineralization studies reported by Gadikota et al. [1].

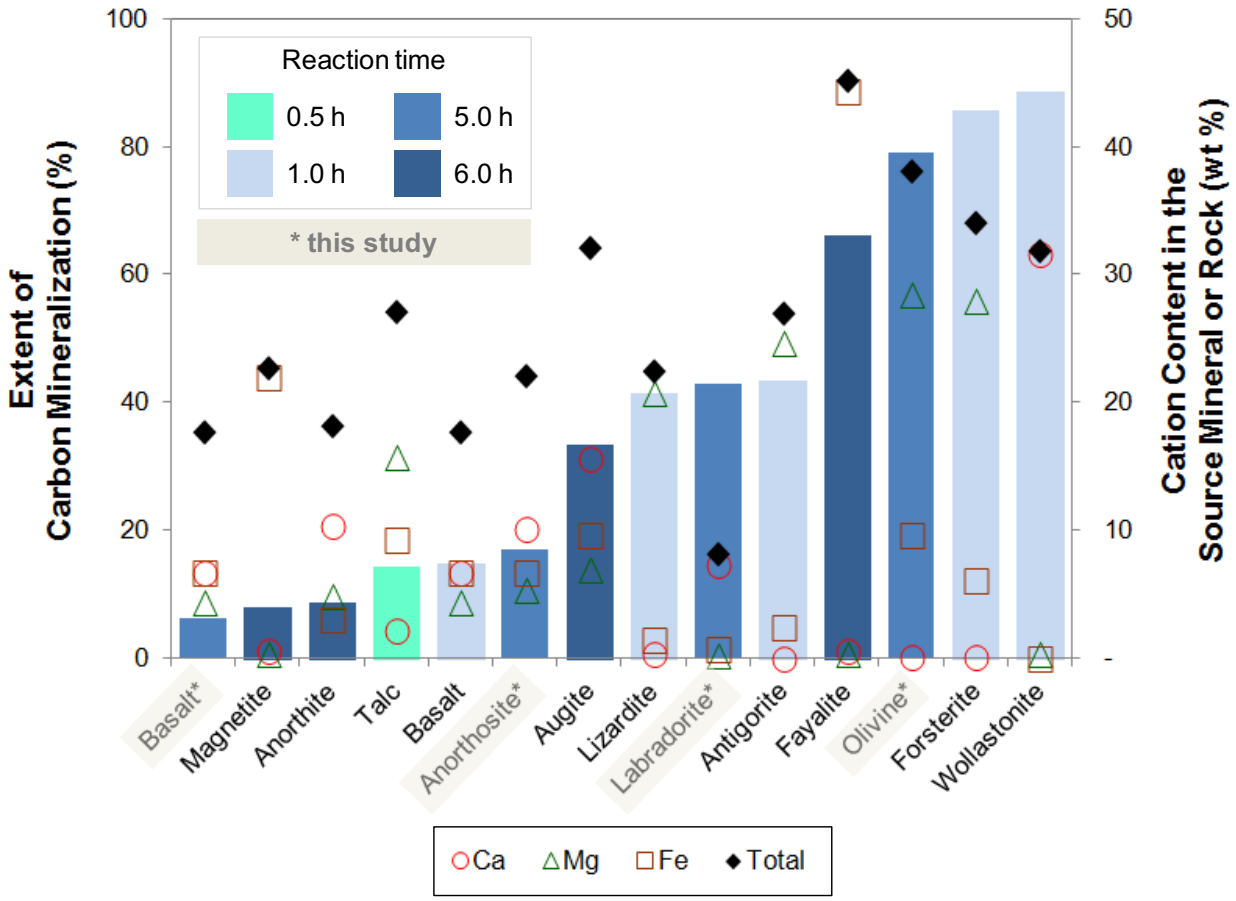

Figure 7. Comparison of the reactivities of various Ca and Mg-bearing minerals and rocks and their CO_2 storage potential. These comprehensive data are from this study (grey colored minerals/rocks), olivine data reported by Gadikota et al.[1] and other data reported by O' Connor and co-workers at NETL-Albany [85]. The experiments at NETL-Albany were performed at 185 °C and P_{CO2} = 150 atm in 1.0 M NaCl + 0.64 M $NaHCO_3$, 15 wt% slurry concentration and a stirring rate of 1000 rpm. Our experiments were also performed under very similar reaction conditions (185 °C, P_{CO2} = 139 atm in 1.0 M NaCl + 0.64 M $NaHCO_3$, 15 wt% slurry concentration and a stirring rate of 800 rpm). The grain sizes of these particles are in the range of 3 – 100 micrometers.

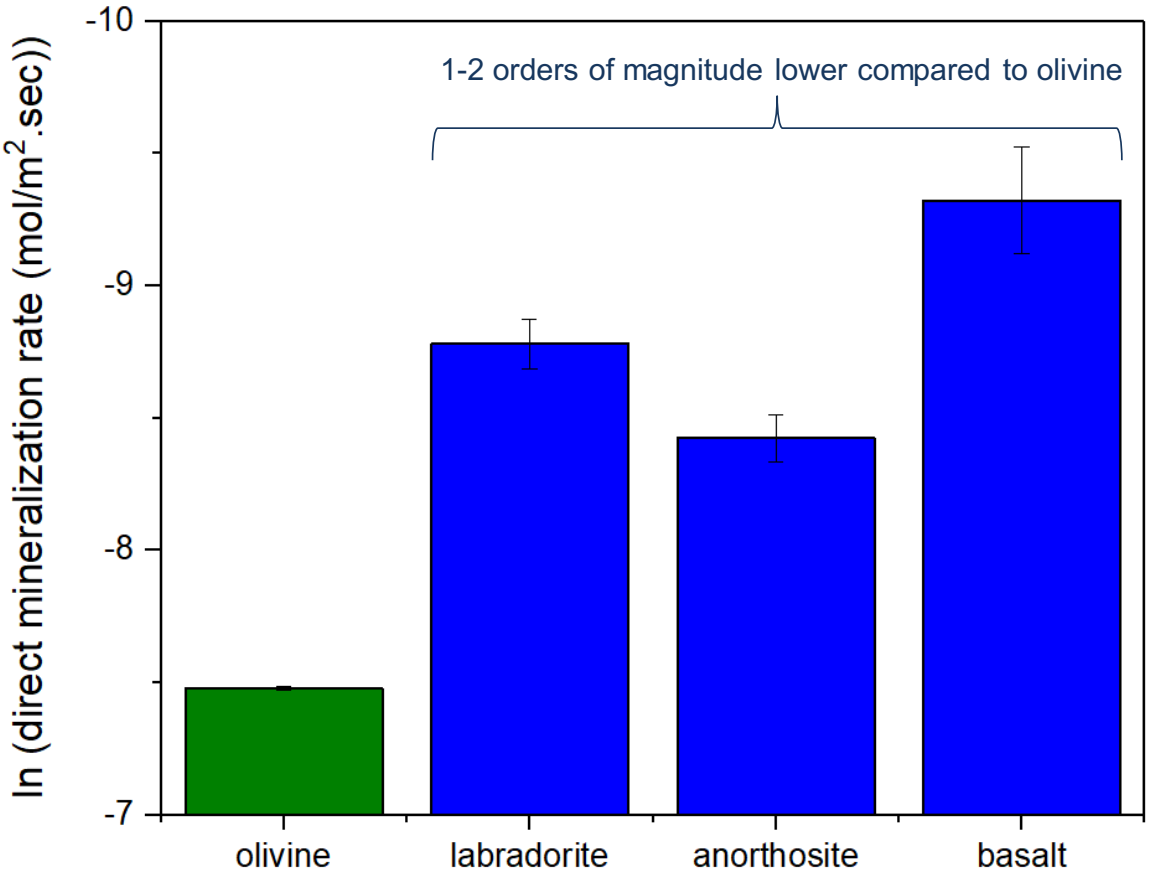

Figure 8. Comparison of the direct carbon mineralization rates of olivine, labradorite, anorthosite, and basalt normalized to the surface area before and after the reaction (see Table 4) as represented by the upper and lower limit bars. The rates reported here represent experiments performed at 185 °C and P_{CO2} = 139 atm in 1.0 M NaCl + 0.64 M $NaHCO_3$ for 3 hours, with 15 wt% slurry concentration and a stirring speed of 800 rpm. Rate data for olivine is based on the extent of carbon mineralization reported by Gadikota et al. [1] and plotted here for comparison.

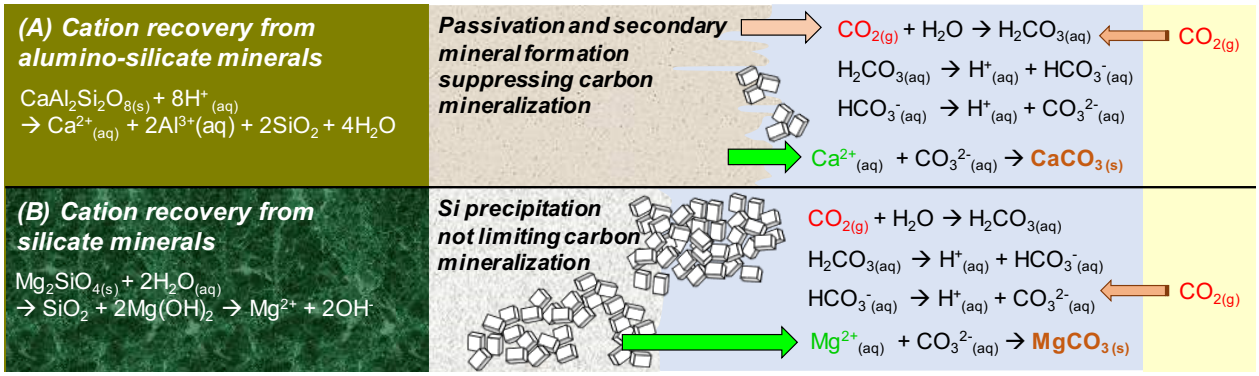

Figure 9. Schematic representation of carbon mineralization with (a) anorthite, $CaAl_2Si_2O_8$ and (b) forsterite, Mg_2SiO_4 at similar experimental conditions of 185 °C, P_{CO2} = 139 atm in 1.0 M NaCl + 0.64 M $NaHCO_3$ in 15 wt% solid for a reaction time of 3 hours.